# cmgh

ORIGINAL RESEARCH

Hepatic SIRT6 Modulates Transcriptional Activities of FXR to Alleviate Acetaminophen-induced Hepatotoxicity

Changhui Liu,[1] Zhisen Pan,[2] Zhouli Wu,[3] Kaijia Tang,[3] Yadi Zhong,[3] Yingjian Chen,[3] Xiaoxia Xiao,[3] Jingyi Guo,[3] Siwei Duan,[3] Tianqi Cui,[3] Guangcheng Zhong,[3] Zifeng Yang,[4] Chong Zhong,[2] Sheng Lin,[5] and Yong Gao[3]

[1]School of Pharmaceutical Sciences, Guangzhou University of Chinese Medicine, Guangzhou, China; [2]The First Affiliated Hospital of Guangzhou University of Chinese Medicine, Guangzhou University of Chinese Medicine, Guangzhou, China; [3]Science and Technology Innovation Center, Guangzhou University of Chinese Medicine, Guangzhou, China; [4]State Key Laboratory of Respiratory Disease, National Clinical Research Center for Respiratory Disease, Guangzhou Institute of Respiratory Health, The First Affiliated Hospital of Guangzhou Medical University, Guangzhou, China; and [5]Key Laboratory of Chinese Internal Medicine of Ministry of Education and Beijing, Dongzhimen Hospital Affiliated to Beijing University of Chinese Medicine, Beijing, China.
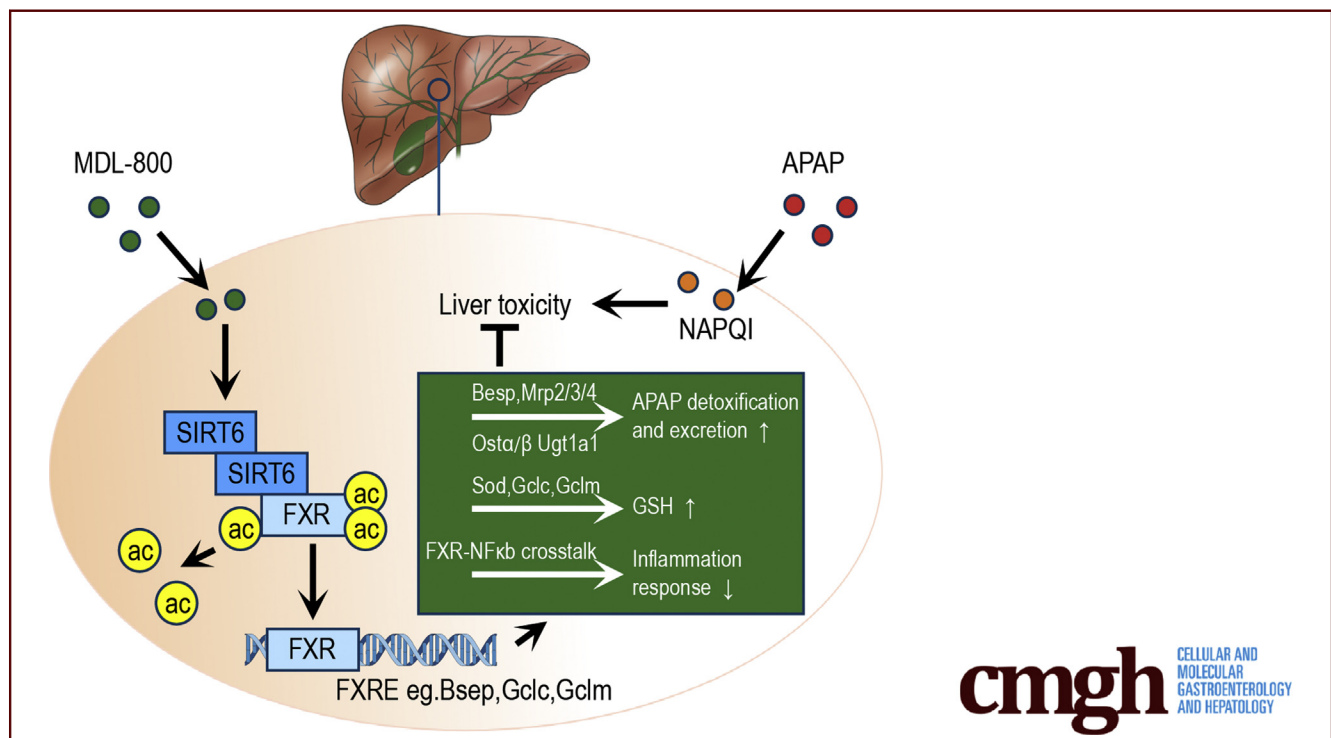
SUMMARY

Acetaminophen (APAP) overdose-caused acute liver failure is a leading public health problem. However, the precise molecular mechanism remains not fully understood. In the present study, we identified a key epigenetic regulator sirtuin 6 (SIRT6) that plays an essential role in attenuating APAP overdose-induced liver injury through up-regulation of FXR-mediated anti-oxidative and anti-inflammatory function, suggesting that SIRT6 may serve as a potential therapeutic target for the treatment of APAP-induced hepatotoxicity.

BACKGROUND & AIMS: Excessive acetaminophen (APAP) intake causes oxidative stress and inflammation, leading to fatal hepatotoxicity; however, the mechanism remains unclear. This study aims to explore the protective effects and detailed mechanisms of sirtuin 6 (SIRT6) in the defense against APAP-induced hepatotoxicity.

METHODS: Hepatocyte-specific SIRT6 knockout mice, farnesoid X receptor (FXR) knockout mice, and mice with genetic or pharmacological activation of SIRT6 were subjected to APAP to evaluate the critical role of SIRT6 in the pathogenesis of acute liver injury. RNA sequences were used to investigate molecular mechanisms underlying this process.

RESULTS: Hepatic SIRT6 expression was substantially reduced in the patients and mice with acute liver injury. The deletion of SIRT6 in mice and mice primary hepatocytes led to high N-acetyl-*p*-benzo-quinoneimine and low glutathione levels in the liver, thereby enhancing APAP overdose-induced liver injury, manifested as increased hepatic centrilobular necrosis, oxidative stress, and inflammation. Conversely, overexpression or pharmacological activation of SIRT6 enhanced glutathione and decreased N-acetyl-*p*-benzo-quinoneimine, thus alleviating APAP-induced hepatotoxicity via normalization of liver damage, inflammatory infiltration, and oxidative stress. Our molecular analysis revealed that FXR is regulated by SIRT6, which is associated with the pathological progression of ALI. Mechanistically, SIRT6 deacetylates FXR and elevates FXR transcriptional activity. FXR ablation in mice and mice primary hepatocytes prominently blunted SIRT6 overexpression and activation-mediated ameliorative effects. Conversely, pharmacological activation of FXR mitigated APAP-induced hepatotoxicity in SIRT6 knockout mice.

CONCLUSIONS: Our current study suggests that SIRT6 plays a crucial role in APAP-induced hepatotoxicity, and pharmacological activation of SIRT6 may represent a novel therapeutic strategy for APAP overdose-induced liver injury. *(Cell Mol Gastroenterol Hepatol 2022;14:271–293;* https://doi.org/10.1016/j.jcmgh.2022.04.011*)*

Keywords: APAP; FXR; Inflammation; Oxidative Stress; SIRT6.

Acetaminophen (APAP) is a commonly used analgesic and antipyretic drug. Under therapeutic dosage, APAP is regarded as safe and effective, but an overdose of APAP can cause potentially fatal acute liver injury (ALI).[1] Following absorption, APAP is transported to the liver for metabolism and biotransformation. In the liver, phase I metabolizing enzymes such as cytochrome p450 2E1 (CYP2E1), CYP3A4, and CYP1A2 mediate the metabolism of APAP to generate reactive N-acetyl-*p*-benzoquinone imine (NAPQI), which can covalently bind to the thiol group of glutathione (GSH) or other proteins, thereby affecting their therapeutic efficacy and leading to toxicity.[1,2] Detoxification of NAPQI is presumably mediated by GSH,[3] and phase II conjugating enzymes (such as UGT1A1 and SULT2A1) that produce glucuronidated and sulfate products, which are subsequently excreted into urine via efflux transporters (such as MRP2, MRP3, MRP4, and BSEP).[4,5] However, hepatic GSH at the normal level cannot tolerate overproduced NAPQI upon APAP overdosing, which leads to the generation reactive oxygen species (ROS), which triggers mitochondrial dysfunction, DNA fragmentation, and cell apoptosis/necrosis.[6,7] Such oxidative stress induced by NAPQI also induces sterile inflammation by elevating the generation of pro-inflammatory cytokines, including tumor necrosis factor (TNF)-α, interleukin (IL)-1β, and IL-6[8,9] and contributes to liver damage or even initiates acute liver failure.[10] Therefore, suppressing excessive oxidative stress and inflammation induced by NAPQI in the liver may represent a good therapeutic strategy against APAP-induced ALI.

As a member of the nicotinamide adenine dinucleotide-dependent histone deacetylases, sirtuin 6 (SIRT6) is able to deacetylate histones onlysine residues (eg, H3K9, and H3K56) and have previously been implicated in the regulation of numerous cellular processes and activities. These include, but are not limited to, cell proliferation/differentiation, aging, cancer, and metabolism.[11–14] In addition, increasing evidence has shown that SIRT6 can regulate the expression of inflammatory genes such as NF-κB and c-Jun by deacetylating H3K9 on the promoters of these genes,[15–17] suggesting that SIRT6 acts as a hepatoprotective gene. We and others have previously reported that SIRT6 ablation in the liver of mice can accelerate high-fat diet-induced hepatic steatosis, alcohol-induced alcoholic liver disease, or carbon tetrachloride (CCl$_4$)/bile duct ligation-induced fibrotic liver, respectively.[12,18–21] In contrast, liver overexpression or pharmacological activation of SIRT6 displays an obvious hepatoprotective effect against liver disease,[12,18–21] unlike other sirtuins (SIRT1 and SIRT3), which have been shown to have protective effects against liver injury.[22–24] However, a p53-induced recruitment of SIRT6 was reported to potentiate APAP-induced hepatocyte damage in AML12 cells,[25] but the in vivo protective effect and mechanism mediated by SIRT6 in APAP-induced acute liver injury are far from clear.

Farnesoid X receptor (FXR, NR1H4) is a nuclear receptor of bile acid-activated transcription factor, which is predominantly expressed in the liver and intestine. Upon activation by its agonist, FXR heterodimerizes with retinoid X receptor and binds to FXR response elements (FXREs), which then regulate the transcription of target downstream genes involved in bile acid synthesis (eg, CYP7A1, CYP8A1, CYP27A1), uptake/transport (NTCP, BSEP, MRP2/3/4, OSTα/β), metabolism (CYP3A4, UGT1A1, SULT2A1), and GSH synthesis (*Gclc*, *Gclm*, and *Sod2*).[26,27] In addition to its regulatory effects on bile acid synthesis and transport, lipid/glucose homeostasis, and xenobiotic metabolism,[28] we and others have recently shown evidence that FXR activation confers significant hepatoprotection against α-naphthylisothiocyanate/CCl$_4$/bile duct ligation-induced liver injury, and high-fat diet-induced nonalcoholic fatty liver disease.[29–31] Furthermore, the hepatoprotective effect of FXR in APAP-induced hepatotoxicity may be attributed to

Most current article

the suppression of oxidative stress and inflammatory responses.[32–34] Together, these results demonstrate a critical function of FXR in liver injury. However, the mechanism underlying the regulation of FXR expression and activity in APAP-induced liver injury needs to be elucidated. Therefore, we developed a model of APAP-induced ALI in SIRT6 hepatocyte-deficient mice and investigated the role of SIRT6 in APAP-induced hepatic injury.

Results

Hepatic SIRT6 Expression is Remarkably Reduced in Human and Murine ALI

To investigate the functional impact of SIRT6 on the progression of ALI, we analyzed SIRT6 expression levels in healthy individuals and patients with disease-associated acute liver failure (ALF). Interestingly, hepatic nuclear SIRT6 protein levels were decreased in patients with disease-associated ALF relative to those of normal controls, and no difference in this trend was observed between males and females (Figure 1, A and B).

To further assess the potential role of SIRT6 in liver injury, we examined hepatic SIRT6 expression in various ALI mouse models induced by overdose of APAP, lipopolysaccharide, and CCl₄. Consistent with the above findings, APAP exposure substantially reduced the expression levels of SIRT6 in the liver at 3, 6, 9, and 12 hours (Figure 1, C and Figure 2, A). A similar decrease was observed in liver samples from mice treated with lipopolysaccharide and CCl₄ (Figure 2, A). In parallel to the APAP-induced mouse model, SIRT6 expression in mice primary hepatocytes (MPHs) was notably decreased after APAP exposure in a time-dependent manner (Figure 1, D and Figure 2, B). Taken together, these results indicate that SIRT6 may be involved in the pathogenesis of human and murine ALI.

Hepatic SIRT6 Deficiency Leads to Deterioration of APAP Overdose-induced ALI

To probe the role of SIRT6 in the development of ALI, we generated hepatocyte-specific SIRT6 knockout (SIRT6-LKO) mice (Figure 4, A). Compared with control mice, hepatic SIRT6 deletion aggravated APAP-induced liver injury, as illustrated by the increased serum alanine transaminase (ALT) and aspartate transaminase (AST) levels, as well as the percentage of liver weight relative to body weight due to aggravated necrosis (Figure 3, A and B). Histopathological morphology also confirmed exacerbated hepatic centrilobular necrosis, accompanied by visible bleeding and liver cell apoptosis in SIRT6-LKO mice after APAP administration (Figure 3, C and D). In conjunction with elevated necrosis, the apoptosis marker, the Bax/Bcl-2 ratio was markedly increased in SIRT6-LKO mice (Figure 3, E). Mechanistically, SIRT6-LKO mice displayed increased hepatic NAPQI levels due to up-regulated CYP3A11 and suppressed OSTβ expression (Figure 3, F and G), whereas genes involved in antioxidants, including Sod2 and Gclc, were decreased in SIRT6-LKO mice, thereby dramatically depleting hepatic GSH and SOD levels, leading to fatal ROS overproduction in the liver (Figure 3, H–J). Consistently,

exposure of SIRT6-deficient MPHs to APAP caused remarkably exacerbated cytotoxicity, as evidenced by elevated ROS generation, cell apoptosis, and reduced GSH levels (Figure 3, K and L, Figure 4, B). Collectively, our results demonstrate that SIRT6 deficiency worsens APAP overdose-induced hepatotoxicity.

Hepatic SIRT6 Deletion Promotes Inflammatory Infiltration in APAP Overdose-induced Mice

To further explore the functional effect of SIRT6 in APAP-induced ALI, we tested whether inflammatory monocytes were involved in the observed exacerbation of APAP-induced hepatotoxicity following SIRT6 deficiency. Of note, we observed a significant increase in inflammatory CD11b/F4/80⁺ monocyte infiltration and serum release of pro-inflammatory cytokines including IL-1β, IL-6, and TNF-α in SIRT6-LKO mice (Figure 5, A and B, Figure 6, A and B). Corresponding to the increased inflammatory infiltration, we found further elevated nuclear NF-κBp65 protein levels in SIRT6-LKO mice relative to SIRT6$^{fl/fl}$ control mice, and resulting in elevated IL-1β, IL-6, and TNF-α mRNA expression levels (Figure 5, C and D, Figure 6, C). Likewise, APAP-treated SIRT6-deficient MPHs caused strikingly elevated inflammation levels, as observed by a further increase in the generation of pro-inflammatory cytokines including IL-6 and TNF-α, along with increased pro-inflammatory gene expression (Figure 5, E and F). Overall, these results suggest that exacerbation of APAP overdose-induced hepatotoxicity following SIRT6 deficiency was associated with deteriorated hepatic infiltration of inflammatory cells.

Genetic or Pharmacological Activation of SIRT6 Prominently Improved APAP Overdose-induced ALI

To confirm the protective role of SIRT6 in APAP overdose-induced hepatotoxicity, we generated liver SIRT6 overexpression mice models with Ad-SIRT6 adenovirus injection via tail vein (Figure 7, A, Figure 8, A). Following treatment with APAP, SIRT6 overexpression mice displayed improved hepatotoxicity, as manifested by the increased survival rate and lower serum parameters including ALT and AST (Figure 7, B and C). In addition, the ratio of liver weight relative to body weight was decreased due to the alleviation of hepatic centrilobular necrosis, as revealed by the histological analysis (Figure 7, D-F, Figure 8, B). Consistently, the ratio of Bax/Bcl-2 was substantially reduced in liver SIRT6 overexpression mice (Figure 7, G). Moreover, hepatic NAPQI levels were notably reduced, whereas GSH was enhanced, leading to a reduction in hepatic ROS generation in Ad-SIRT6-infected mice (Figure 7, H-J). Gene expression profile analysis revealed that liver SIRT6 overexpression resulted in an inhibitory expression of CYP2E1 and CYP3A11, whereas UGT1A11, OSTβ, NTCP, and MRP2 gene expressions were increased, which benefits APAP detoxification (Figure 7, K and L). Moreover, anti-oxidative genes, including SOD2 and Gclc, were upregulated by SIRT6 overexpression (Figure 7, M).
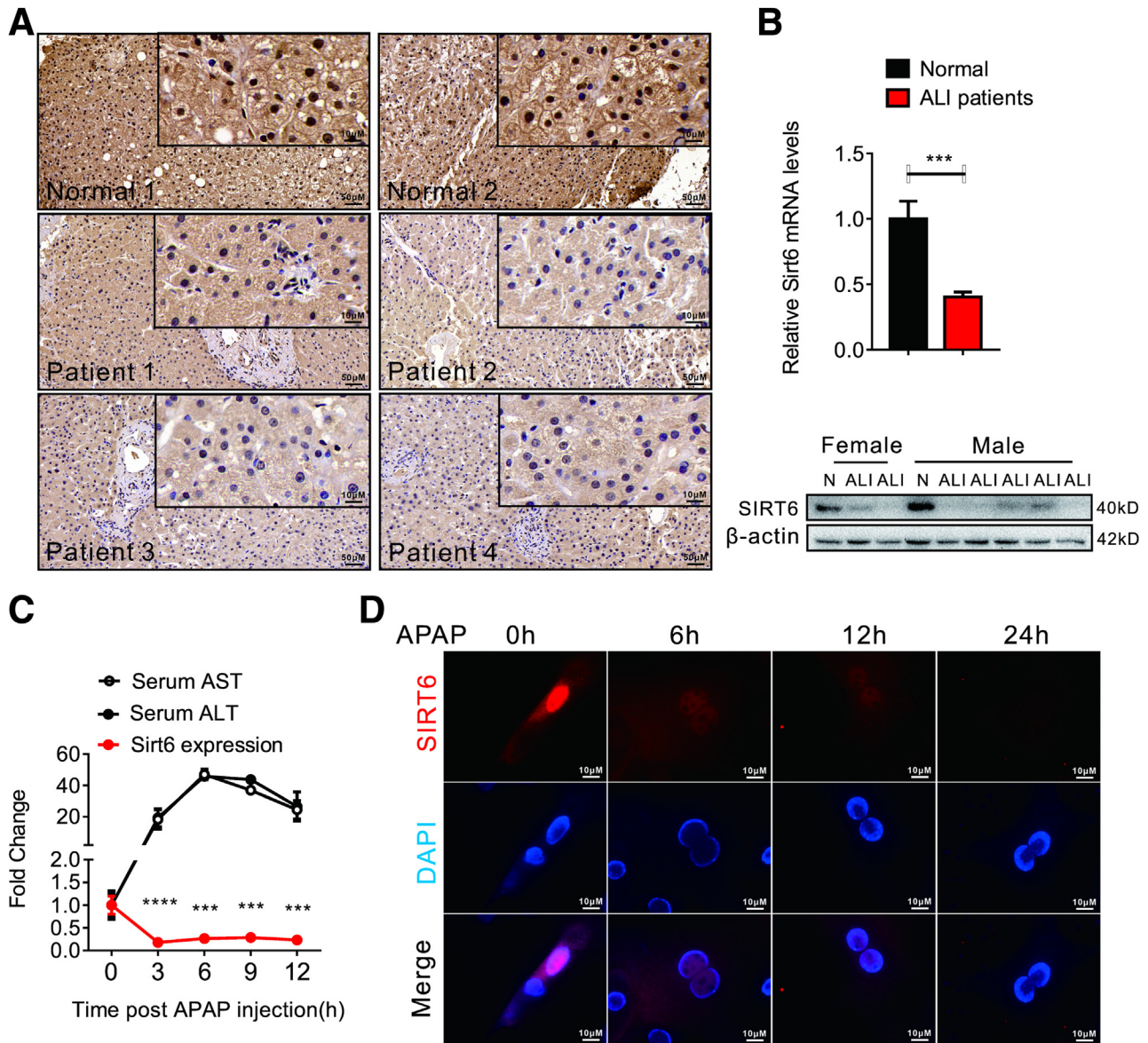
Figure 1. Hepatic SIRT6 expression is significantly reduced in human and murine acute injured liver. (*A*) The protein expression of SIRT6 in liver biopsies and preoperative testing for obstructive jaundice-induced liver injury was measured using immunohistochemical assay, and hematoxylin was used to determine the nuclei; (*B*) The mRNA and protein levels of SIRT6 were reduced in liver sections of obstructive jaundice-induced liver injury (n = 7); (*C*) The mRNA levels of SIRT6 at different time intervals following APAP injection were determined using quantitative polymerase chain reaction (n = 6); (*D*) Immuno-fluorescence staining showed a significant reduction of SIRT6 in MPHs after APAP treatment. Data are means ± standard error of the mean. *$P < .05$, **$P < .01$, ***$P < .001$. Similar results were observed in 3 independent experiments.

Hepatic pro-inflammatory cytokine generation analysis also demonstrated a decrease in TNF-α, IL-1β, and IL-6 (Figure 9, *A*, Figure 10, *A*). Liver SIRT6 overexpression also evidently blocked NF-κBp65 nuclear translocation (Figure 9, *B*, Figure 10, *B*), thereby leading to repression of TNF-α gene expression and reduction of inflammatory infiltration via inhibition of hepatic F4/80 and CD11b expression (Figure 9, *C* and *D*). In agreement, MPHs infected with Ad-SIRT6 displayed a prominent ameliorative effect on APAP-induced liver cytotoxicity, as revealed by the elevated GSH level and lower ROS generation and cell apoptosis (Figure 9, *E-G*, Figure 10, *C*). Furthermore, SIRT6

overexpression also protected against APAP-induced cellular inflammation, as evidenced by the reduced release of pro-inflammatory cytokines and suppression of pro-inflammatory gene expression (Figure 9, *H*, Figure 10, *D*).

To address the important role of SIRT6 deacetylase activity in hepatoprotection against APAP-induced liver injury, a mutant SIRT6 adenovirus (Ad-SIRT6(H133Y)) with deficient deacetylase activity obtained by disrupting the deacetylase domain of SIRT6 was constructed as previously described.[18,35] Interestingly, Ad-SIRT6(H133Y) infection failed to reverse the APAP-induced hepatotoxicity, as revealed by the unchanged ratio of liver weight relative to
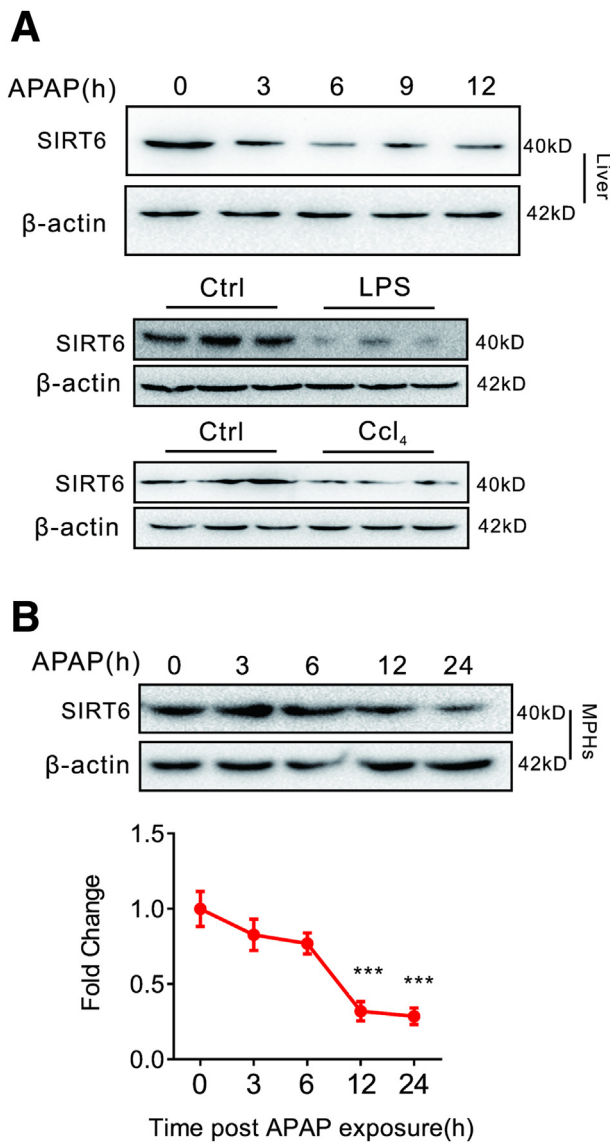
Figure 2. Hepatic SIRT6 expression is reduces in acute injured liver and MPHs. (*A*) The protein expression of SIRT6 in liver sections of mice treated with APAP, lipopolysaccharide (LPS), and CCl4; (*B*) APAP treatment decreased the expression of SIRT6 in MPHs in a time-dependent manner.

body weight and serum ALT and AST levels (Figure 11, *A* and *B*). Moreover, deficiency of SIRT6 deacetylase activity marginally caused hepatoprotective effects against APAP-induced hepatotoxicity in mice injected with Ad-mSIRT6 compared with mice injected with Ad-ctrl, as demonstrated by compromised hepatoprotection of SIRT6 activation in the suppression of liver cell apoptosis, hepatic inflammation, oxidative stress, liver cell apoptosis, and APAP detoxification (Figure 11, *C–J*).Taken together, our study revealed the importance of SIRT6 deacetylase activity in protection against APAP-induced hepatotoxicity.

We then validated whether pharmacological activation of SIRT6 could improve liver injury. Mice were intraperitoneally injected with MDL-800, a recently identified SIRT6 allosteric activator. Following MDL-800 administration,

APAP-induced hepatotoxicity was effectively suppressed based on serum biochemical and liver histological analysis, as well as an improved liver cell apoptosis (Figure 12, *A-D*). MDL-800 administration also significantly enhanced antioxidative genes and NAPQI detoxifying genes, leading to a decrease in NAPQI generation and an improvement in hepatic ROS accumulation (Figure 12, *E*, Figure 13, *A* and *B*). Moreover, MDL-800 administration substantially reduced APAP-induced NF-κBp65 nuclear translocation and decreased pro-inflammatory cytokine release via inhibition of their gene expression (Figure 12, *F-H*).

To further elucidate the importance of SIRT6 in mediating MDL-800-derived hepatoprotection against APAP-induced liver injury, hepatocyte-deficient SIRT6 mice were treated with MDL-800. Consistently, SIRT6 deletion significantly diminished the protective effects of MDL-800 against APAP-induced hepatotoxicity, as revealed by the unaltered serum TNF-α, ALT, and AST levels, and liver cell apoptosis, accompanied by an unchanged CD11b/F480 level (Figure 14, *A-C*). Taken together, these data suggest that genetic or pharmacological activation of SIRT6 in the liver could effectively alleviate APAP overdose-induced ALI.

SIRT6 Interacts With FXR and Activates its Transcriptional Activity

To further explore the mechanism of SIRT6-induced protective effects against ALI, we performed RNA sequencing (RNA-seq) from livers of Ad-GFP or Ad-SIRT6 infected mice after APAP exposure, and our data indicated that 388 genes were changed in accordance with SIRT6 overexpression, with 171 upregulated and 217 downregulated genes (Figure 15, *A*). GO analysis suggested that the inflammatory response and superoxide dismutase activity signaling pathways were altered (Figure 15, *B*). Likewise, genes involved in APAP metabolism and inflammation were significantly changed, especially those involved in FXR signaling, which has been shown to play an essential role in the pathological progression of APAP-induced ALI via regulation of inflammation and oxidative stress (Figure 15, *C*).

We next studied the molecular mechanism by which SIRT6 regulates FXR signaling. Consistently, our quantitative polymerase chain reaction data confirmed that genetic or pharmacological activation of SIRT6 effectively upregulated the expression of FXR and its target genes, Shp and Bsep (Figure 15, *D*). Previous studies have indicated that FXR acetylation plays critical roles in maintaining stability, preventing degradation, and regulating its target gene transcriptional activity.[15,36] However, whether APAP treatment affects acetylation levels have not yet been explored. Thus, we evaluated FXR deacetylation by SIRT6 in MPHs after transfection of cells with Ad-SIRT6. Co-immunoprecipitation assays revealed a direct physical interaction between FXR and SIRT6, which led to the deacetylation and stability of FXR to activate this pathway, whereas the upregulation of FXR and Bsep was diminished in Ad-SIRT6(H133Y)-infected MPHs (Figure 15, *E-G*, Figure 16, *A*). Indeed, we observed a remarkable increase in FXR-luc
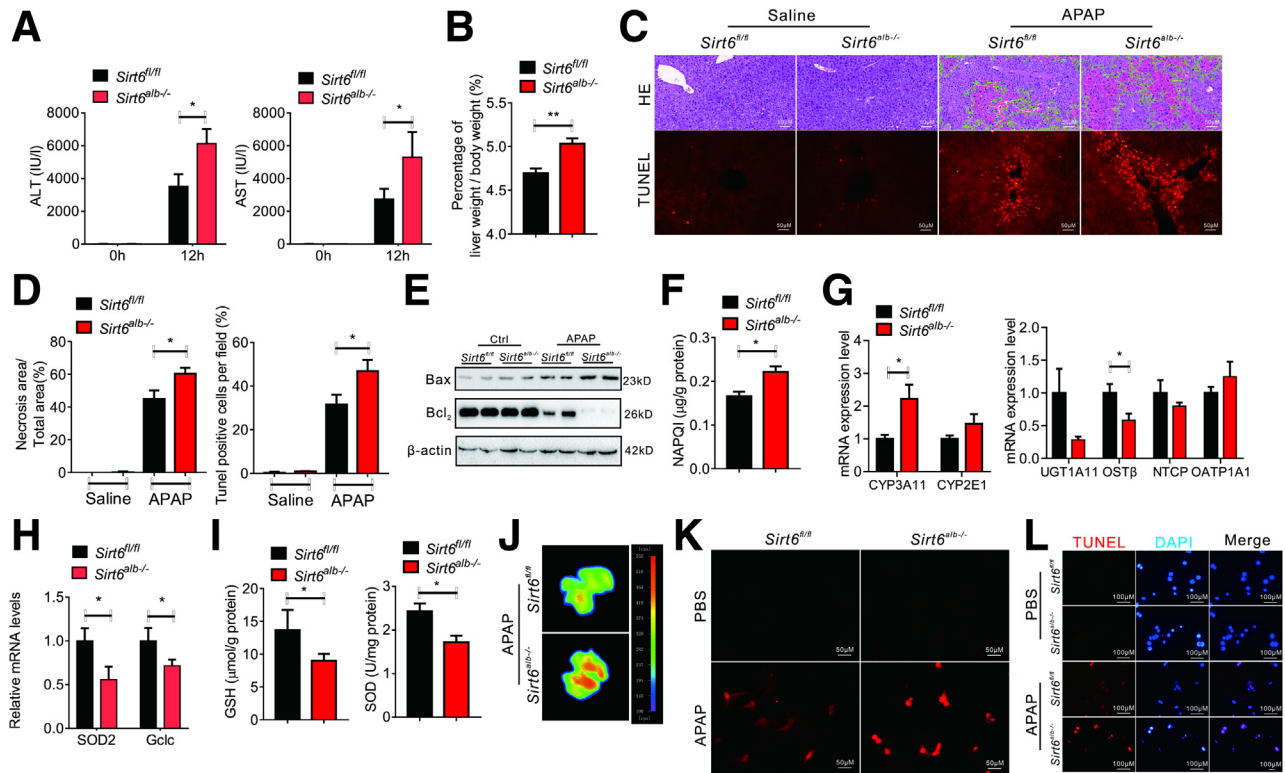
Figure 3. Hepatic SIRT6 deficiency deteriorates APAP overdose-induced acute liver injury. Occurrences at 12 hours following APAP injection. (*A*) Serum ALT and AST levels of SIRT6-LKO and control mice after APAP injection; (*B*) SIRT6-LKO mice displayed higher ratio of liver weight relative to body weight after APAP injection; (*C* and *D*) H&E and TUNEL assay showed deteriorated centrilobular necrosis and liver cell apoptosis in SIRT6-LKO mice after APAP administration; (*E*) Western blotting indicated an increased rate of hepatic Bax relative to Bcl2 expression in SIRT6-LKO mice after APAP administration; (*F*) ELISA assay showed increased NAPQI levels in APAP-treated SIRT6-LKO mice; (*G*) Hepatic SIRT6 knockout leads to change of genes involved in APAP metabolism; (*H*) Hepatic SIRT6 deficiency decreased the expression of anti-oxidative genes including SOD2 and Gclc; (*I*) Hepatic GSH and SOD levels were reduced in SIRT6-LKO mice after APAP treatment; (*J*) Hepatic ROS levels were increased in SIRT6-LKO mice after APAP treatment; (*K* and *L*) SIRT6 deletion leads to elevated ROS generation and cell apoptosis in MPHs. Data are means ± standard error of the mean; n = 6 to 8 mice/group. *P < .05, **P < .01, ***P < .001. Similar results were obtained in 3 independent experiments.

activity after SIRT6 overexpression (Figure 16, *B*). FXR is a constitutive transcription factor of the nuclear receptor that binds to FXRE in the promoter region of its target gene to regulate its transcriptional activity. We further confirmed that SIRT6 enhanced the transcriptional activity of BSEP-luc using a luciferase reporter assay (Figure 16, *C*), suggesting
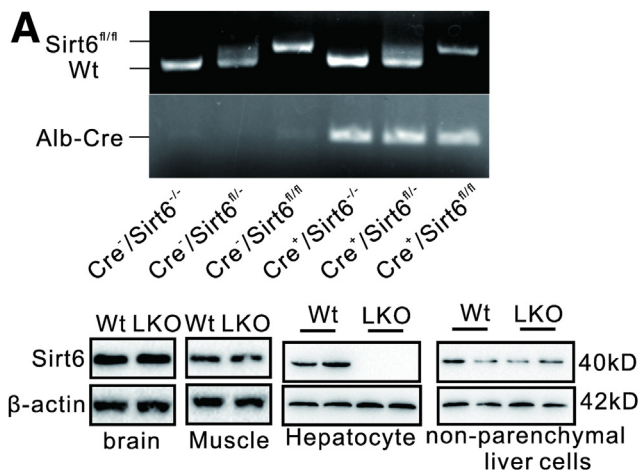

Figure 4. Genotyping of hepatocyte SIRT6 deficient mice and GSH levels in MPHs. (*A*) Genotyping of hepatic SIRT6 deletion mice and Wb data showed the deletion of SIRT6 in hepatocytes. (*B*) Hepatocyte GSH levels were decreased in Sirt6 deficiency MPHs after 12 hours post APAP injection. Data are means ± standard error of the mean; n = 6 per group. *P < .05, **P < .01, ***P < .001. Similar results were observed in 3 independent experiments.
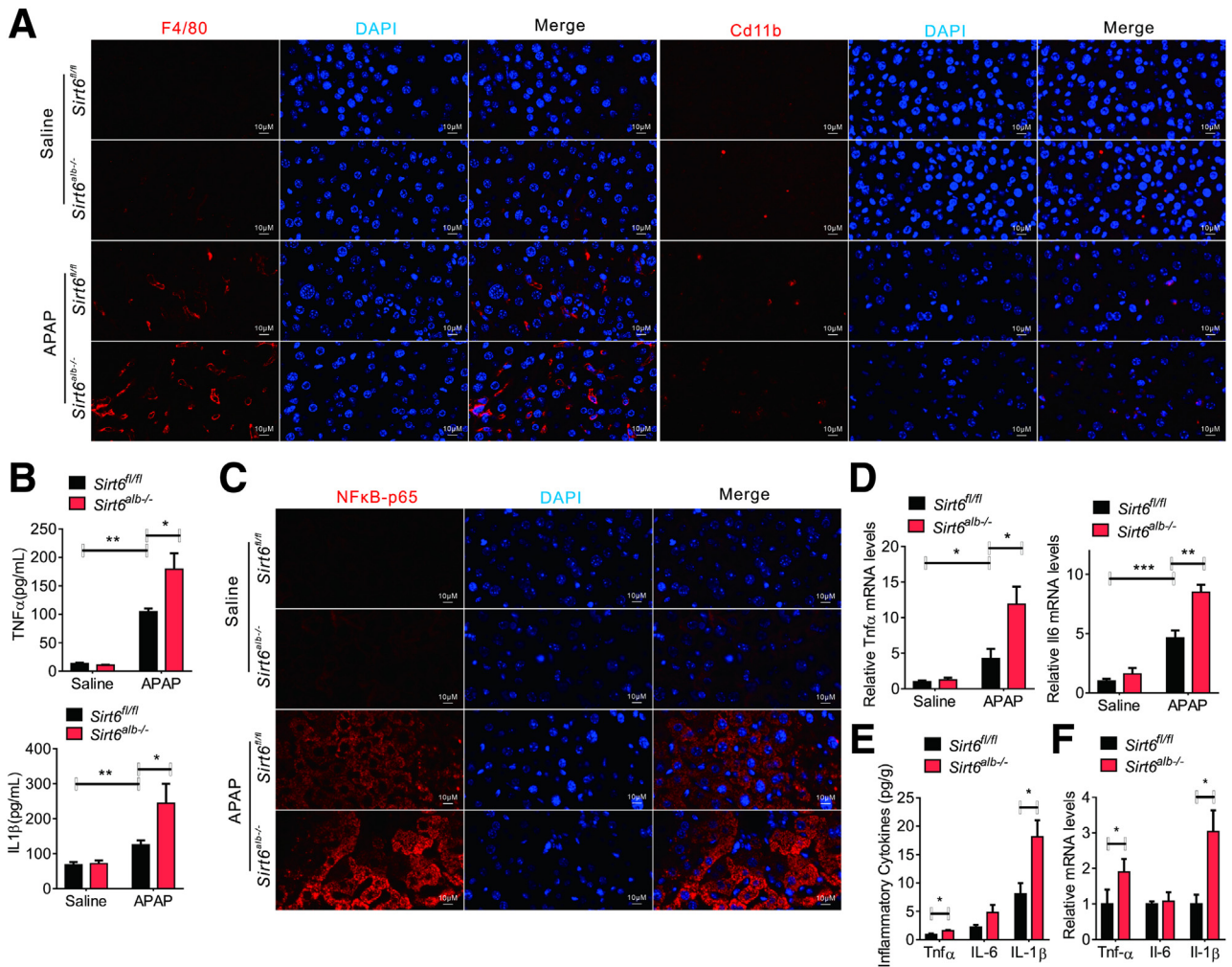
Figure 5. Hepatic SIRT6 deletion promotes inflammatory infiltration in APAP overdose-induced mice. Occurrences at 12 hours following APAP injection. (*A*) The protein levels of F4/80 and CD11b were determined using immunofluorescence, and the nuclei were stained with DAPI; (*B*) ELISA assay showed an increase in serum pro-inflammatory cytokines including IL-1β and TNF-α in SIRT6-LKO mice after APAP injection; (*C* and *D*) Nuclear NF-κBp65 protein level (*C*) and TNF-α mRNA level (*D*) were elevated in SIRT6-LKO mice after APAP treatment; (*E* and *F*) SIRT6 deletion increased the expression of pro-inflammatory genes (*E*) and cytokine release (*F*) in MPHs. Data are means $\pm$ standard error of the mean; n = 6 to 8 mice/group. *$P < .05$, **$P < .01$, ***$P < .001$. Similar results were obtained in 3 independent experiments.

that FXR may act as a candidate target for SIRT6-mediated protective function.

Taken together, our results revealed that SIRT6 can reduce cytotoxicity by deacetylating FXR to enhance FXR protein stabilization and FXR transcriptional activity.

FXR Deficiency Compromises Genetic or Pharmacological SIRT6 Activation-mediated Hepatoprotective Effects Against APAP Overdose

Subsequently, we explored whether the protective effects of SIRT6 are dependent on FXR in APAP-induced liver necrosis, oxidative stress, and inflammatory response in vivo. The global deletion of FXR mice (FXR-KO) and wild-type (WT) mice were injected with Ad-SIRT6 adenovirus via the tail vein, and then exposed to APAP. Compared with WT mice, FXR-KO mice exhibited a compromised amelioration of APAP-induced hepatotoxicity, as revealed by the high serum ALT and AST levels, along with profound centrilobular necrosis and ROS generation (Figure 17, *A-C*). In parallel, hepatic NAPQI levels were relatively high, whereas GSH and SOD levels were lower in FXR-KO mice, even when injected with Ad-SIRT6 adenovirus (Figure 17, *D-F*). Consistently, the protective role of SIRT6 in inflammation was also impaired in FXR-KO mice, as indicated by a significantly high level of pro-inflammatory cytokine production and extensive inflammatory infiltration (Figures 17, *G* and *H*). A similar detrimental effect was observed in MDL800-treated mice in which FXR deletion mostly abrogated the protective effects of MDL-800 treatment (Figure 17, *I-N*, Figure 18, *A* and *B*). Consistent with the in vivo results, FXR knockout partly abrogated SIRT6 overexpression-mediated hepatoprotective effects against
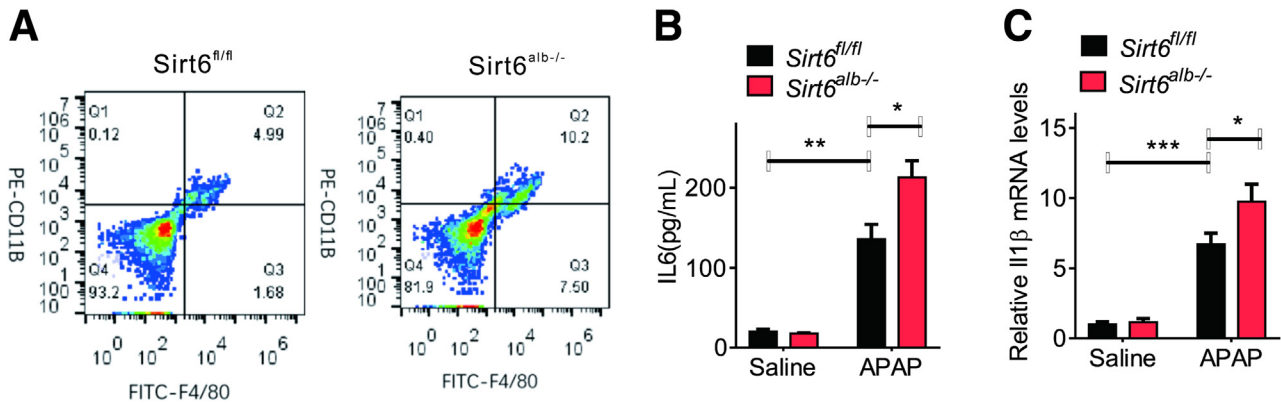
Figure 6. Hepatic SIRT6 deletion worsens inflammatory infiltration in APAP overdose-induced mice. (*A*) Flow cytometry assay showed a significant increase in inflammatory CD11b/F4/80$^+$ monocyte infiltration; (*B*) ELISA assay showed an increase of serum IL-6 in SIRT6-LKO mice after 12 hours post APAP injection; (*C*) The expression of IL-1β in SIRT6-LKO mice after 12 hours post APAP injection. Data are means $\pm$ standard error of the mean; n = 6 to 8 mice/group. *$P <$ .05, **$P <$ .01, ***$P <$ .001.

inflammatory response, oxidative stress, and liver cell apoptosis, as evidenced by the decrease in NF-κBp65 protein expression, ROS generation, and terminal deoxynucleotidyl transferase dUTP nick end labeling (TUNEL) levels in MPHs (Figure 18, *C*). These data suggest that FXR deficiency can blunt the genetic and pharmacological activation of SIRT6-mediated protection against APAP overdose-induced hepatotoxicity.

FXR Activation Mitigated APAP-induced Deteriorative Hepatotoxicity in Hepatocyte-specific SIRT6 Deficiency Mice

To further validate the role of FXR in mediating the effect of SIRT6 in ALI, SIRT6-LKO mice were orally administered obeticholic acid (OCA), a typical FXR agonist, for 5 days, followed by APAP administration. Compared with vehicle treatment, OCA pretreatment can effectively reverse SIRT6 deficiency-mediated hepatotoxicity induced by APAP, as indicated by lower serum ALT and AST levels, accompanied by an improvement in pro-inflammatory cytokine generation, including TNF-α and IL-6 (Figure 19, *A-C*). Moreover, OCA-induced FXR activation effectively alleviated APAP-induced hepatic centrilobular necrosis and liver apoptosis in SIRT6-LKO mice (Figure 19, *D*). Overall, our results revealed that the hepatoprotective effects of SIRT6 are dependent on FXR activation during the development of oxidative stress, necrosis, apoptosis, and inflammatory response after APAP overdose in the liver of mice.

Discussion

In the present study, we have revealed a critical role of SIRT6 in the inhibition of inflammatory response and oxidative stress against APAP overdose-induced hepatotoxicity using both animal and MPH cell models. Our study started with the finding that hepatic SIRT6 expression is significantly reduced in patients with disease-associated ALF and in the models of MPH cells and ALI mice with overdose of APAP treatment. Using mouse models of

hepatocyte-specific SIRT6 knockout or overexpression, we confirmed that hepatocyte-specific SIRT6 deficiency can enhance the hepatotoxicity induced by an APAP overdose, whereas mice with SIRT6 overexpression are prominently resistant to APAP overdose-induced liver injury. The results indicated that hepatic SIRT6 levels were related to the severity of APAP-induced liver injury. Similarly, SIRT6 activation by a small molecule significantly alleviated APAP-induced ALI in mice. Mechanistically, SIRT6 is able to deacetylate and stabilize FXR, thus promoting FXR transcriptional activity. More importantly, FXR deficiency displayed impaired hepatoprotective effects in mice with SIRT6 activation either through genetic or pharmacological approaches, providing proof of concept that SIRT6 overexpression and activation may represent a novel therapeutic approach for the treatment of APAP-induced ALI.

Once administered, APAP is rapidly absorbed by intestine and transferred to the liver. The conversion of APAP to the reactive metabolite NAPQI by CYP2E1 and CYP3A4 represents the initial step of liver injury. NAPQI can react with GSH, thus depleting the most important cellular redox regulator GSH,[2,7] leading to oxidative stress. On these bases, it is not difficult to explain why suppressing CYP2E1 and CYP3A4 activity in the liver can lead to reduced hepatic toxicity upon high-dose APAP treatment.[37,38] We found that changing hepatocyte SIRT6 levels affected the hepatic expression of CYP2E1 and CYP3A4 during APAP-induced liver injury, suggesting that hepatocyte SIRT6 is a regulator ofAPAP metabolism. In contrast, hepatocyte SIRT6-deficient mice showed high levels of NAPQI in the liver during APAP-induced liver injury. One possible explanation is that hepatic SIRT6 deficiency is associated with the decreased efflux transport of NAPQI, as indicated by the result that SIRT6 deficiency can reduce the expression of efflux transporters, such as BSEP, MRP2, and OSTα/β, which are involved in the hepatic NAPQI elimination pathway.[39,40] In parallel, mice with liver overexpression or pharmacological activation of SIRT6 demonstrated an elevated expression of efflux transporters and a relatively lower
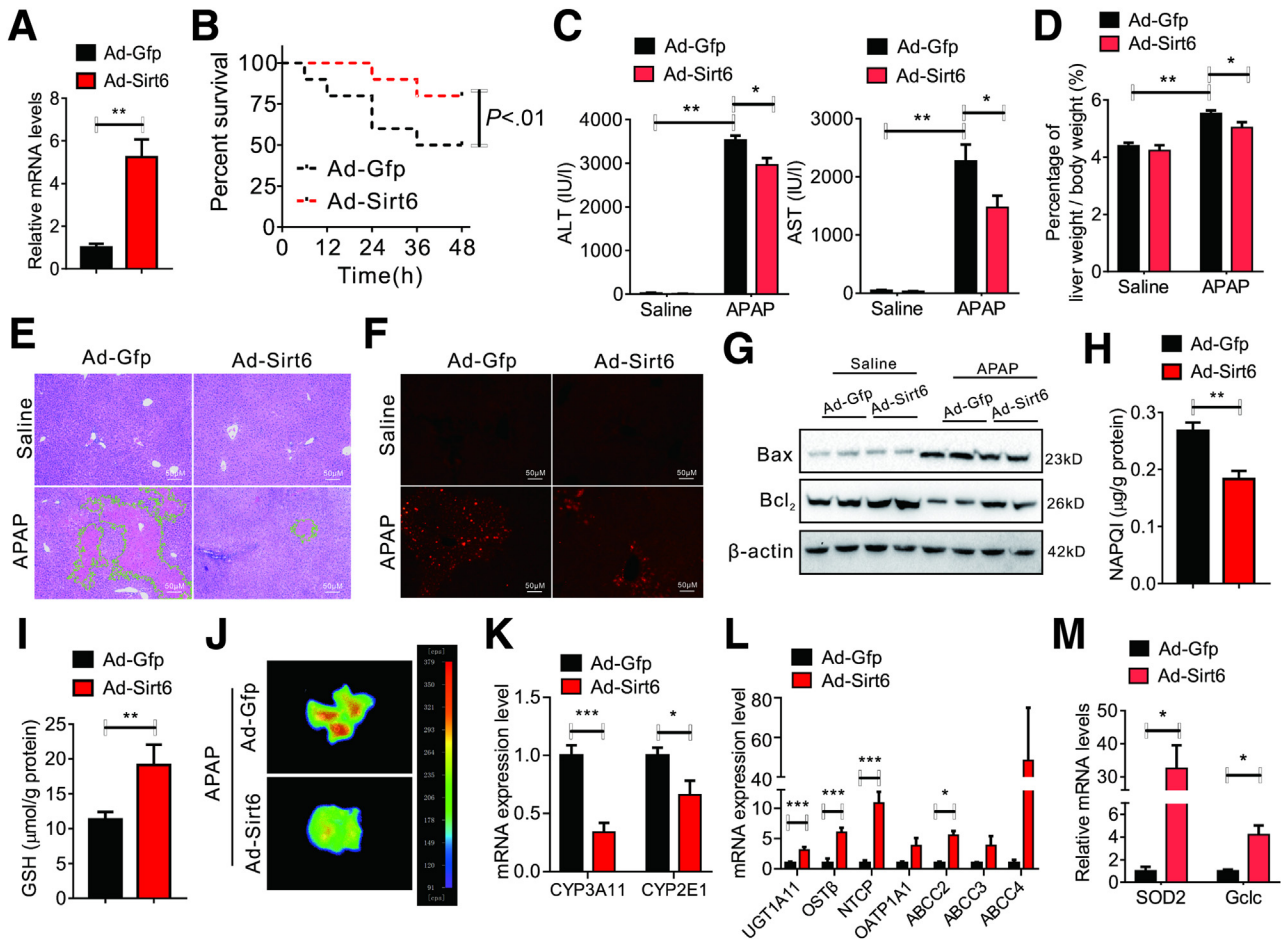
Figure 7. SIRT6 overexpression prominently improves APAP overdose-induced acute liver injury. Occurrences at 12 hours following APAP injection. (*A*) Quantitative polymerase chain reaction data showed a hepatic overexpression of SIRT6 in Ad-SIRT6-infected mice; (*B*) SIRT6 overexpression increased the survival rate after indicated time of APAP injection; (*C*) SIRT6 overexpression decreased serum ALT and AST levels after APAP treatment; (*D*) SIRT6 overexpression reduced the ratio of liver weight relative to body weight in APAP-injected mice; (*E* and *F*) APAP-induced centrilobular necrosis (*E*) and liver cell apoptosis (*F*) were improved in Ad-SIRT6-infected mice; (*G*) SIRT6 overexpression decreased the ratio of hepatic Bax relative to Bcl2 expression; (*H*) ELISA assay showed a decrease of NAPQI levels in Ad-SIRT6-infected mice; (*I* and *J*) Hepatic GSH (*I*) and ROS (*J*) levels were decreased in Ad-SIRT6-infected mice after APAP treatment; (*K* and *L*) Hepatic SIRT6 overexpression altered genes involved in APAP metabolism; (*M*) Hepatic SIRT6 overexpression increased anti-oxidative genes including SOD2 and Gclc. Data are means ± standard error of the mean; n = 6 to 8 mice/group. *P < .05, **P < .01, ***P < .001. Similar results were obtained in 3 independent experiments.

Figure 8. SIRT6 overexpression decreases APAP overdose-induced necrosis. After 12 hours post APAP injection, (*A*) Wb data showed overexpression of SIRT6 in Ad-Sirt6 infected mice; (*B*) Quantification of necrosis area and tunnels positive cells in ad-Sirt6- or ad-Gfp-infected mice after APAP treatment. Data are means ± standard error of the mean; n = 6 to 8 mice/group. *P < .05, **P < .01, ***P < .001.
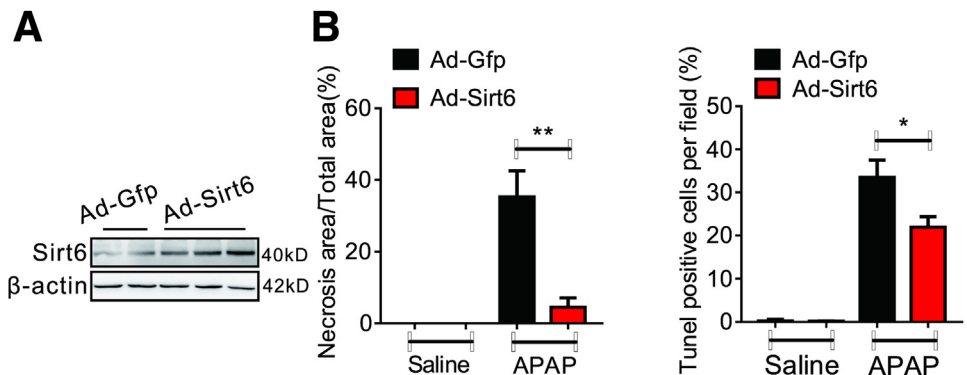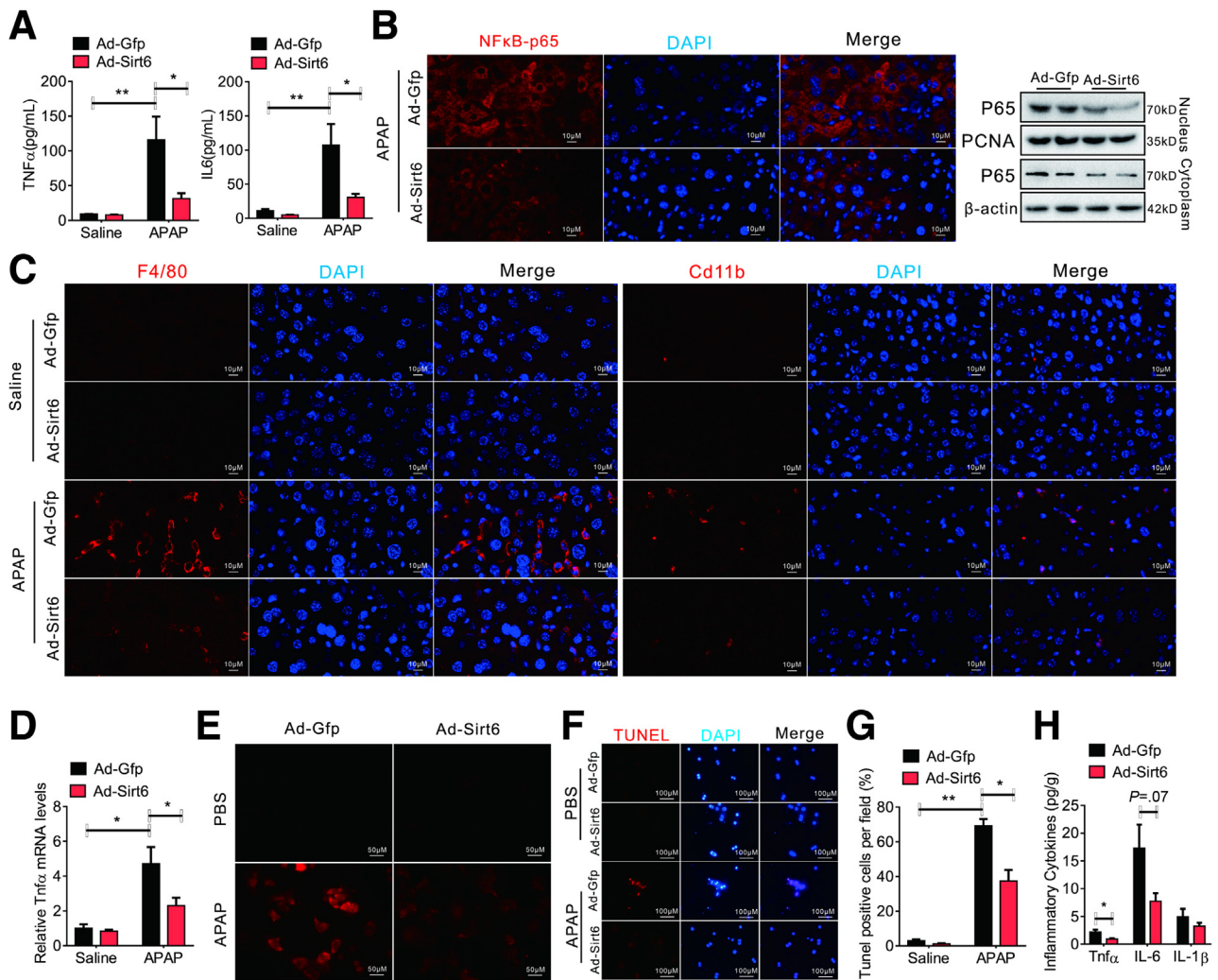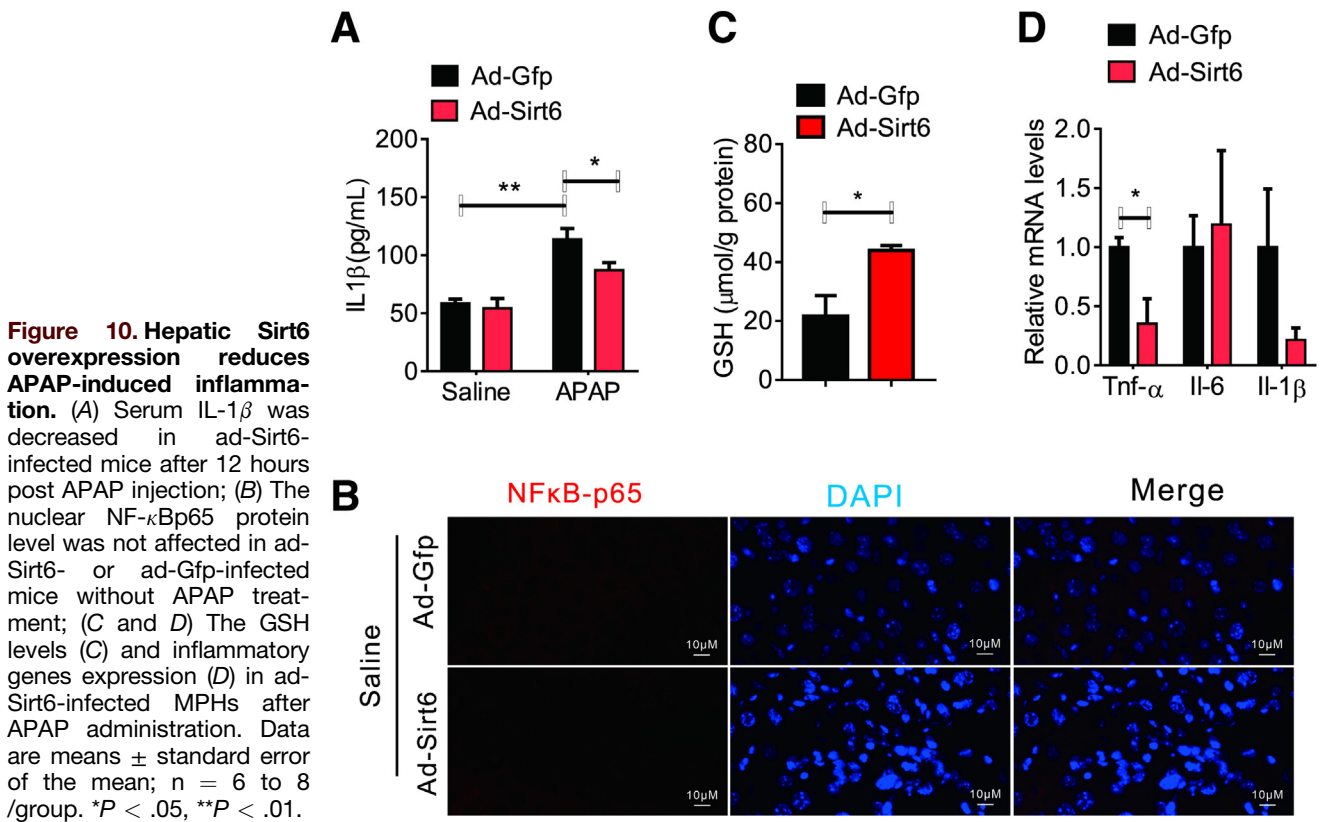
Figure 9. Hepatic SIRT6 overexpression suppresses inflammatory infiltration after APAP treatment. Occurrences at 12 hours following APAP injection. (A) Serum pro-inflammatory cytokine including TNF-α and IL-6 were decreased in Ad-SIRT6-infected mice after APAP injection; (B) SIRT6 overexpression decreased nuclear NF-κBp65 protein level; (C) Immunofluorescence data indicated that the protein levels of F4/80 and CD11b were decreased in Ad-SIRT6-infected mice after APAP injection; (D) SIRT6 overexpression increased GSH levels in MPHs; (E–G) SIRT6 overexpression decreased ROS (E) and cell apoptosis (F and G) in MPHs; (H) SIRT6 overexpression decreased pro-inflammatory cytokine release in MPHs. Data are means ± standard error of the mean; n = 6 to 8 mice/group. *$P < .05$, **$P < .01$, ***$P < .001$. Similar results were obtained in 3 independent experiments.

NAPQI level in the liver. Our hypothesis is partially supported by He et al, who report displayed that SIRT6 overexpression promoted cholesterol efflux by increasing the expression of efflux transporters ABCA1 and ABCG1.[41] Moreover, another possible explanation is that hepatic SIRT6 deficiency led to the suppression of the detoxification process of NAPQI by downregulating UGT1A1 mRNA, thereby impeding excretion of NAPQI to urine. There is evidence that increased UGT1A1 mRNA levels and enzymatic activity are related to enhanced APAP urinary clearance and protective function against APAP-induced injury.[42,43] We observed that liver SIRT6 overexpression resulted in elevated UGT1A1 mRNA levels in the liver, which are associated with low NAPQI levels, underlining a central role of SIRT6 in mediating APAP detoxification through phase II conjugating enzymes. Together, the decreased hepatic NAPQI levels in mice mediated by liver overexpression or pharmacological activation of SIRT6 may be relevant to the elevated expression of efflux transporters and phase II metabolizing enzymes.

After GSH depletion, additional NAPQI binds to cellular and mitochondrial proteins, causing mitochondrial dysfunction and oxidative stress. As an essential detoxification factor, GSH can affect the onset and recovery of APAP-induced liver injury.[44] SIRT6 plays a critical role in redox signaling in the liver, and its downregulation is closely related to enhanced oxidative stress via excessive ROS generation,[16,19] implying that the maintenance of normal SIRT6 levels is important to reduce APAP-induced liver damage. Similar to the report by Kim et al,[19] we found that

Figure 10. Hepatic Sirt6 overexpression reduces APAP-induced inflammation. (A) Serum IL-1β was decreased in ad-Sirt6-infected mice after 12 hours post APAP injection; (B) The nuclear NF-κBp65 protein level was not affected in ad-Sirt6- or ad-Gfp-infected mice without APAP treatment; (C and D) The GSH levels (C) and inflammatory genes expression (D) in ad-Sirt6-infected MPHs after APAP administration. Data are means ± standard error of the mean; n = 6 to 8/group. *$P < .05$, **$P < .01$.

hepatocyte SIRT6-deficient mice showed low levels of GSH, which is relevant to the reduced mRNA levels of *Gclc, Gclm*, and *Sod2*, which encode GSH synthesis enzymes. However, liver overexpression of SIRT6 or pharmacological activation of SIRT6 by MDL-800 can remarkably enhance liver GSH levels by upregulating the expression levels of these genes, subsequently leading to attenuation of APAP-induced hepatotoxicity. These results suggest that SIRT6-mediated GSH generation may serve as a vital contributor to the prevention APAP-induced liver injury. Indeed, our hypothesis was supported by Zhou et al,[25] who showed that SIRT6 knockdown could inhibit the activation of NRF2, a master regulator of the antioxidant defense system, and NRF2's downstream gene expression in the AML12 cell model, thereby being responsible for worsening APAP-induced hepatotoxicity.[25] However, in contrast to the in vitro results of Zhou et al, we revealed the hepatoprotective effect of SIRT6 against APAP-induced liver injury in mouse model. The hepatoprotective mechanism of SIRT6 against APAP-induced liver injury in mice was, in part, associated with the regulation of FXR expression and transcriptional activity. Therefore, the discrepancy between the hepatoprotective mechanism of SIRT6 in vitro and in vivo needs to be further investigated.

It is known that NAPQI-induced hepatotoxicity and subsequent excessive inflammatory innate responses are the main factors inducing acute liver damage.[45] Indeed, massive neutrophil and macrophage infiltration into liver is regarded as a hallmark of APAP-mediated acute liver inflammation.[10] Therefore, suppressing the infiltration of inflammatory monocytes is, at least partially, an effective therapeutic strategy against APAP-induced inflammatory injury. In the present study, we indicated for the first time that loss of SIRT6 in hepatocytes resulted in amplified infiltration of inflammatory monocytes during APAP treatment, as manifested by the increased expression of hepatic F4/80 and CD11b. As a result, NF-κB signaling is activated, and the levels of pro-inflammatory cytokines (eg, IL-1β, IL-6, and TNF-α) in the liver and serum were increased, thereby accelerating liver inflammatory injury. In contrast, such a negative regulatory pattern of SIRT6 in NF-κB-mediated inflammation response was not observed in SIRT6$^{fl/fl}$ control mice. Liver overexpression or pharmacological activation of SIRT6 can notably reduce APAP-induced inflammatory monocyte recruitment, subsequently abating liver inflammatory injury via inhibition of NF-κB nuclear translocation. Our findings are confirmed by several recent reports, in which they demonstrated that SIRT6 deficiency increased the number of neutrophils and macrophages, thereby enhancing inflammation-mediated activation of hepatic stellate cells.[19,21,46] Similarly, several studies have recently revealed that HDACs including SIRT6 and the acetylation of STAT1 and NF-κBp65 play essential roles in the regulation of NF-κB transcriptional activity,[15,47] thus attenuating inflammation. Our study proved that SIRT6 plays a vital anti-inflammatory role by restricting NF-κB target gene promoters or abating inflammatory signaling molecules, in APAP-induced inflammatory liver damage.[15]
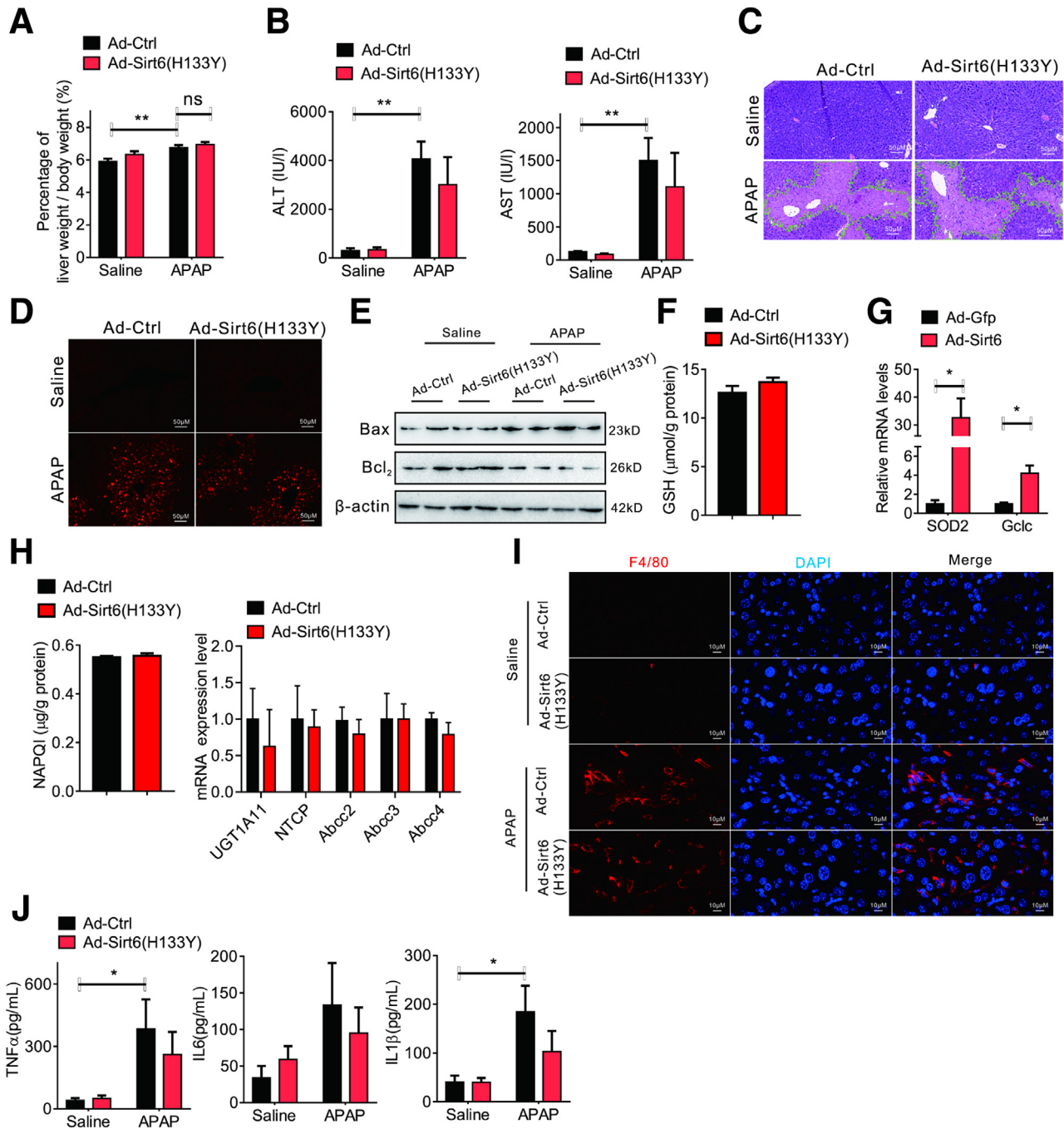
Figure 11. Mutant SIRT6 deacetylase domain fails to alter APAP-induced liver injury. Occurrences at 12 hours following APAP injection, (*A*) liver percentage and (*B*) serum ALT and AST levels in Ad-Ctrl- or Ad-Sirt6 (H133Y)-infected mice after APAP injection; (*C* and *D*) H&E and TUNEL assay showed no change of centrilobular necrosis and liver cell apoptosis in Ad-Sirt6 (H133Y) mice after APAP administration. (*E*) Western blotting indicated no change of hepatic Bax relative to Bcl2 expression in Ad-Sirt6 (H133Y) mice after APAP administration. (*F–H*) No change of GSH levels (*F*), hepatic antioxidantive genes expression (*G*), NAPQI and APAP-metabolism related genes expression (*H*). (*I* and *J*) Mutant SIRT6 deacetylase domain failed to alter change the expression of hepatic F4/80 and serum inflammatory cytokines levels. Data are means ± standard error of the mean; n = 6 to 8 /group. *$P < .05$, **$P < .01$.

Therefore, genetic or pharmacological activation of SIRT6 in the liver can block NF-κB nuclear translocation and mitigate its transcriptional activity, thus attenuating the release of pro-inflammatory cytokines by suppressing the recruitment of inflammatory monocytes in the liver.

We found that SIRT6 overexpression or activation is critical in decreasing oxidative stress and inflammation by promoting NAPQI excretion and detoxification by upregulating the expression of efflux transporters (eg, Bsep and MRP2) and phase II metabolizing enzymes, respectively.
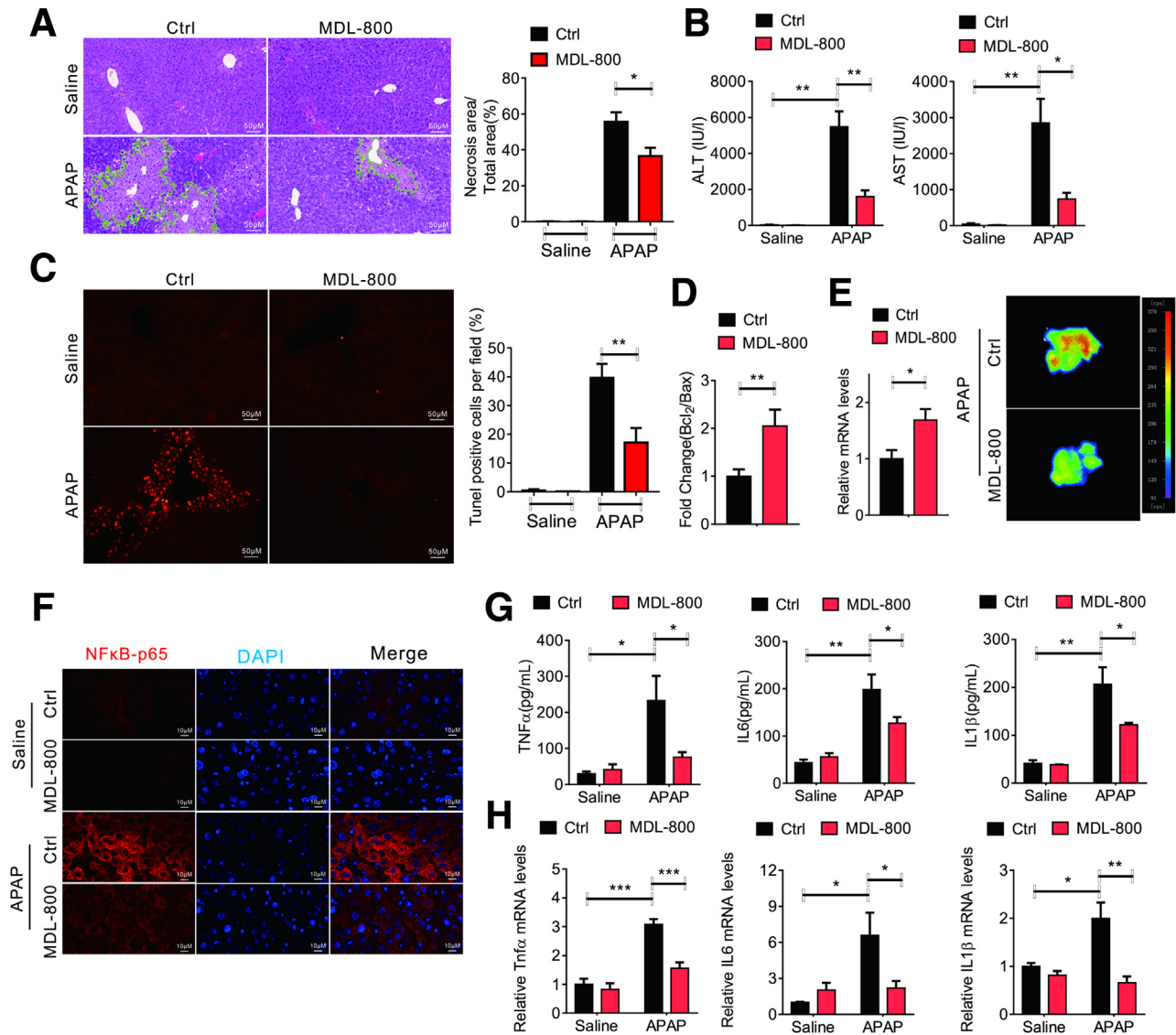
Figure 12. Pharmacological activation of SIRT6 improves APAP overdose-induced acute liver injury. Occurrences at 12 hours following APAP injection. (*A*) MDL-800 treatment decreased hepatic centrilobular necrosis levels after APAP treatment; (*B*) MDL-800 treatment reduced serum ALT and AST levels after APAP treatment; (*C* and *D*) MDL-800 treatment decreased liver cell apoptosis (*C*) and the ratio of Bax relative to Bcl$_2$; (*E*) MDL-800 administration increased hepatic SOD2 expression and decreased hepatic ROS levels after APAP treatment; (*F*) MDL-800 treatment decreased nuclear NF-κBp65 protein levels after APAP treatment; (*G* and *H*) MDL-800 treatment decreased pro-inflammatory cytokine release (*G*) and gene expression (*H*) . Data are means ± standard error of the mean; n = 6 to 8 mice/group. *$P < .05$, **$P < .01$, ***$P < .001$. Similar results were obtained in 3 independent experiments.

Meanwhile, SIRT6 can elevate GSH generation by inducing the expression of antioxidant genes (eg, Gclc, Gclm, and Sod2) and attenuate the infiltration of inflammatory monocytes by inhibiting NF-κB-mediated inflammatory signaling. However, the precise molecular mechanisms involved remain unknown. To address these regulatory mechanisms, RNA-seq analysis was performed. We found that liver overexpression of SIRT6 is related to the activation of the FXR signaling pathway, as evidenced by the elevated expression of its target genes, including SHP and BSEP. Indeed, we and others have previously corroborated the protective effect of FXR against APAP-induced hepatotoxicity mainly via regulation of oxidative stress and

inflammation.[32–34,48] As a bile acid receptor, FXR activation is associated with the regulation of genes encoding bile acid synthesis (eg, CYP7A1, CYP8B1, and CYP27A1), uptake (eg, NTCP and OATPs), transport/excretion (eg, BSEP, MRP2/3/4, and OSTα/β), and detoxification (eg, UGT1A1, and SULT2A1),[32,33] all of which are related to detoxification and excretion of APAP. On the other hand, FXR activation also contributes to enhanced GSH levels via induction of the synthesis enzymes (*Gclc*, *Gclm*, and *Sod2*),[32,33] which are also involved in decreasing NAPQI-induced liver toxicity. Moreover, the direct interaction between FXR and NF-κB confers critical anti-inflammatory features of FXR in hepatoprotection.[49,50] Based on the fact that SIRT6 together
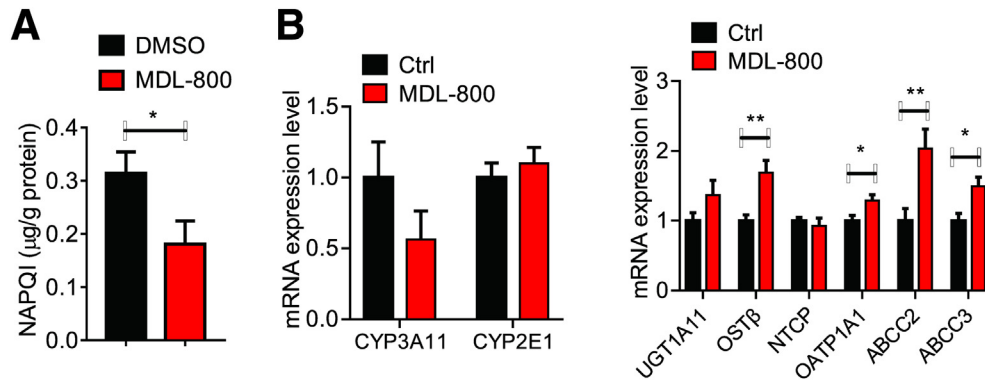
Figure 13. Pharmacological activation of Sirt6 affects APAP metabolism. (*A* and *B*) MDL-800 treatment changed hepatic NAPQI levels (*A*) and genes involved in APAP metabolism (*B*). Data are means ± standard error of the mean; n = 6 to 8 mice/group. *P < .05.

with FXR regulates APAP-induced hepatotoxicity by decreasing oxidative stress and inflammation, and more importantly, hepatic overexpression or pharmacological activation of SIRT6 can potentiate FXR expression level, it cannot be assumed that SIRT6 may regulate FXR activity. SIRT6 possesses histone deacetylase activity, which normally functions as a transcriptional repressor by deacetylating H3K9 and H3K56 on histones that bind the promoters of genes.[18,51] Here, we show that SIRT6 can deacetylate FXR, subsequently elevating FXR expression and reinforcing its transcriptional activity, which reveals the function of SIRT6 in direct activation of gene regulation. The deacetylation level of FXR has been shown to be important for its transcriptional activity.[52,53] The regulatory pattern identified by us is similar to the regulatory mode of SIRT6 to PPARα,[12] in which SIRT6 activates PPARα activity via NCOA2 K780 deacetylation.[12] SIRT6 interacts with FXR followed by binding with FXRE in an FXR-dependent manner and then induces transcription of FXR genes downstream, suggesting that FXR may serve as a downstream gene of SIRT6. Analogously, hepatocyte SIRT1 affects the activity of FXR largely through transcriptional regulation.[36,54,55] Our results indicate that the hepatoprotective effect of liver SIRT6 is strikingly impaired in FXR-deficient mice, which further confirms the critical role of FXR in SIRT6-mediated hepatoprotection against APAP-induced liver injury. In contrast, hepatic FXR activation by OCA can rescue SIRT6 deficiency-mediated deterioration of liver damage induced by APAP. These results reveal a crucial role for theSIRT6-FXR axis in the regulation of APAP-induced hepatotoxicity. However, 2 other possibilities regarding the regulation of FXR by SIRT6 cannot be rigorously excluded in the current study. First, SIRT6 harbors the well-known LXXLL motif in its coactivator domain, which is commonly found in FXR-binding coactivators, possibly influencing the conformation of binding pocket SIRT6 when binding to FXR, thus enabling the increased binding recruitment of FXR coactivators. Second, SIRT6 may activate FXR via deacetylation and activation of a member of the FXR complex, such as a coactivator acetyltransferase (eg, p300, C/EBPα). Therefore, the precise mechanism by which SIRT6 regulates the transcriptional activity of FXR requires further investigation.

In conclusion, we found an important role of SIRT6 in APAP-induced hepatotoxicity. Hepatocyte-specific SIRT6 deficiency in mice aggravates hepatic oxidative stress and inflammatory damage induced by APAP overdose. APAP-induced liver injury can potentially be attributed to the inhibition of the FXR signaling pathway. However, liver overexpression and pharmacological activation of SIRT6 in mice can lead to significant protective effects against APAP-induced hepatotoxicity via attenuation of hepatic oxidative stress and inflammation. Mechanistically, SIRT6 can deacetylate FXR and subsequently increase FXR transcriptional activity, thereby promoting NAPQI excretion, enhancing hepatic GSH levels and suppressing the recruitment of inflammatory monocytes. In addition, mice with FXR deletion exhibited obvious resistance to SIRT6-mediated protective effects against APAP overdose, in both liver overexpression and MDL800 activation models. In contrast, FXR activation by OCA in mice with hepatocyte-specific SIRT6 deficiency clearly improved APAP-induced hepatotoxicity. Therefore, our study demonstrates that specifically targeting hepatocyte SIRT6 or the SIRT6-FXR axis may be a promising therapeutic strategy for APAP-induced ALI.

Methods
Clinical Tissues Preparation

Liver samples from biopsy and preoperative testing for obstructive jaundice-induced acute liver injury were collected from the First Affiliated Hospital of Guangzhou University of Chinese Medicine as previously reported.[56] Written informed consent was obtained from all patients involved in this study. The protocol for clinical tissue preparation was approved by the ethics committees of the First Affiliated Hospital of Guangzhou University of Chinese Medicine (No: ZYYECK(2019)008) and subject to the guidelines of the 1975 Declaration of Helsinki.

Animal Models

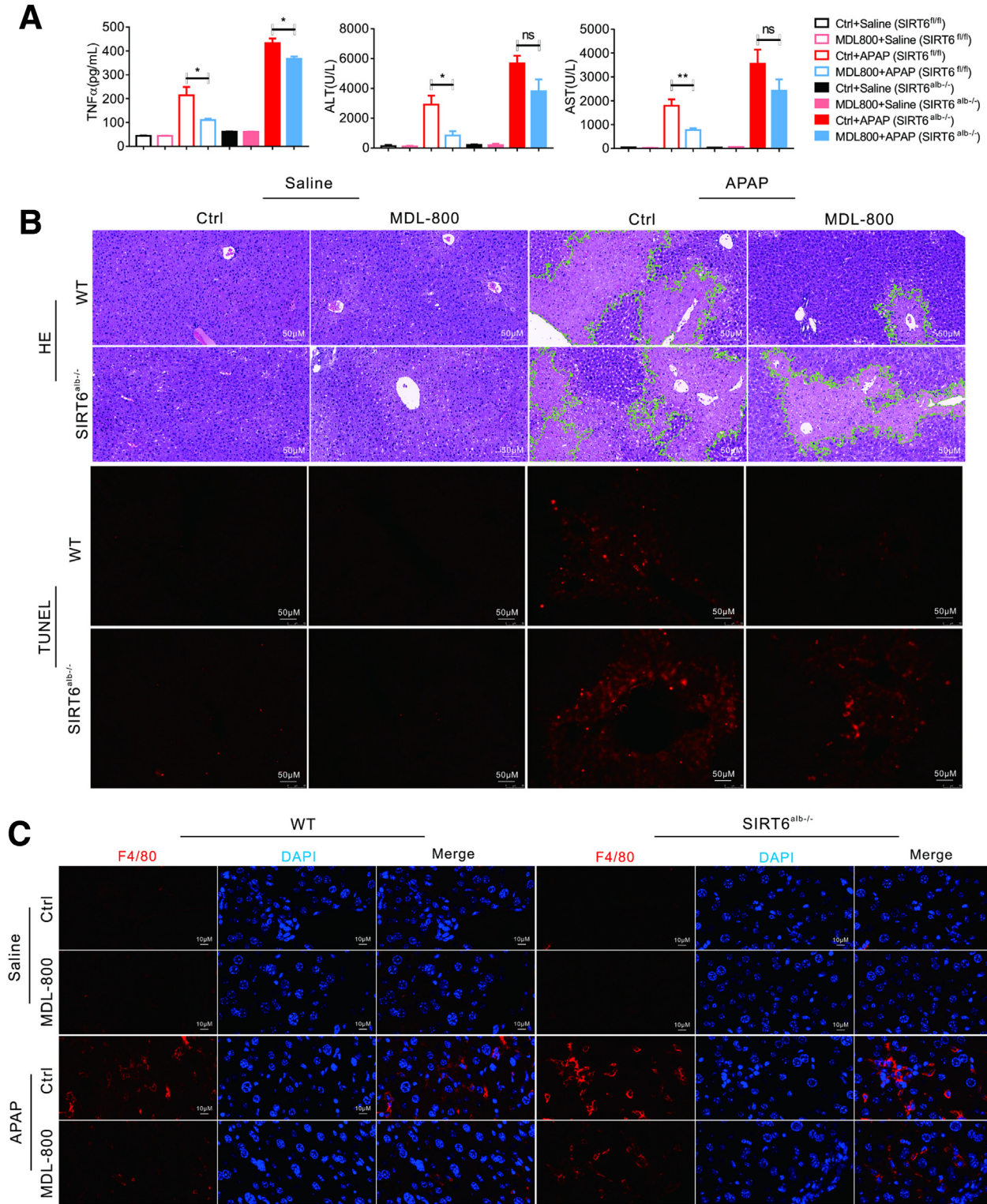Male C57BL/6J mice aged 6 to 8 weeks were purchased from the Model Animal Research Center of Guangzhou

Figure 14. SIRT6 deletion diminishes MDL-800-induced protective effects against APAP treatment. Occurrences at 12 hours following APAP injection. (*A*) Serum TNF-α, ALT, and AST levels in SIRT6 knockout and control mice treated with or without APAP. (*B*) H&E and TUNEL assay showed no change of centrilobular necrosis and liver cell apoptosis in MDL-800 treated SIRT6-LKO mice after APAP administration. (*C*) MDL-800 failed to alter change the expression of hepatic F4/80 in SIRT6-LKO mice treated with or without APAP. Data are means $\pm$ standard error of the mean; n = 6 to 8 /group. *$P <$ .05, **$P <$ .01.
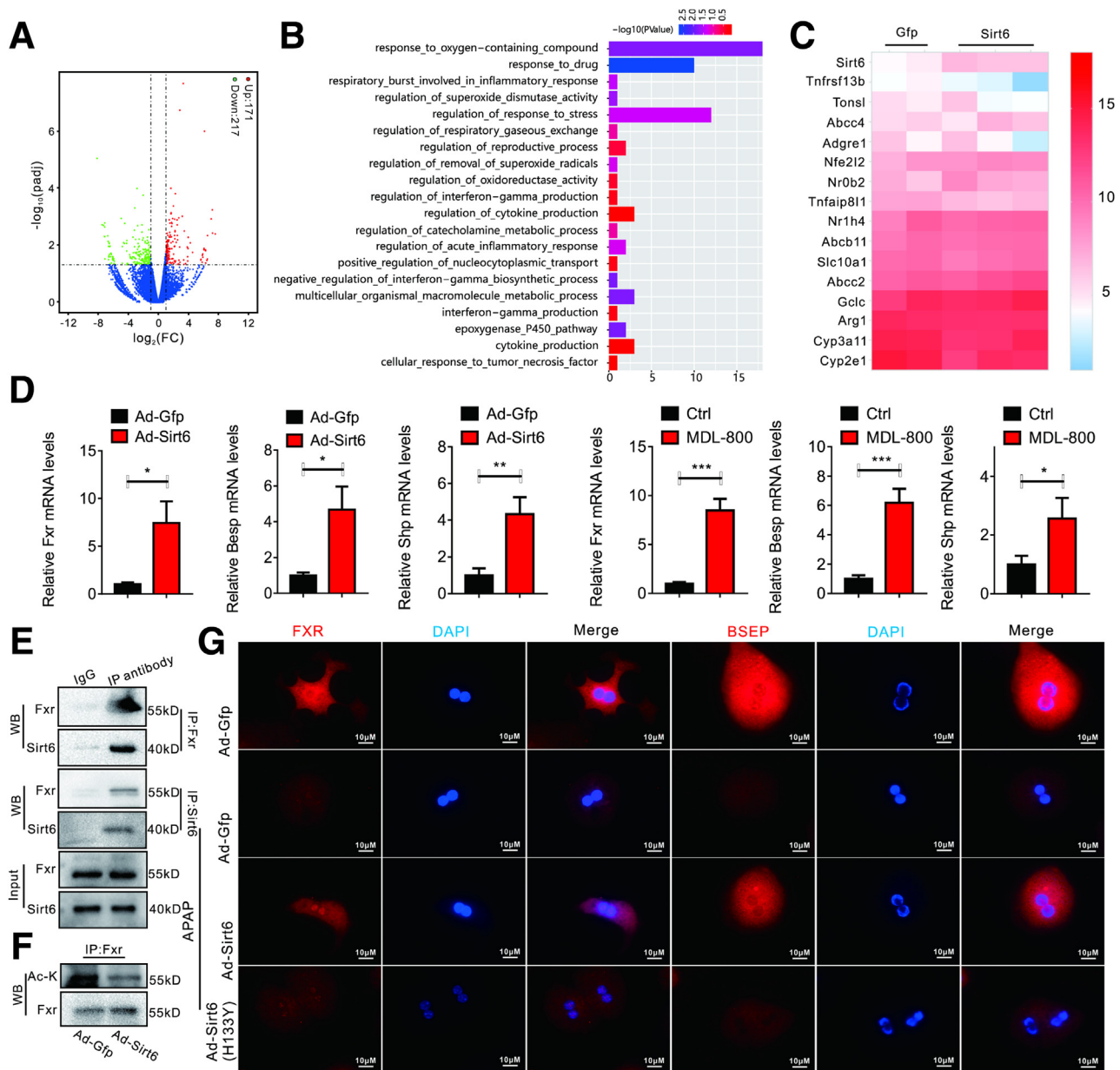
Figure 15. SIRT6 directly interacts with FXR and activates its transcriptional activity. (*A–C*) RNA-seq from livers of ad-Gfp- or ad-SIRT6-infected mice after 12 hours APAP exposure; (*D*) Genetic or pharmacological activation of SIRT6 increased the expression of FXR and its target genes following 12 hours post APAP injection; (*E*) Co-immunoprecipitation assay indicated a direct interaction of FXR and SIRT6; (*F*) SIRT6 overexpression decreases the acetylation of FXR; (*G*) Immunofluorescence data showed that SIRT6 overexpression upregualted FXR and its target gene dependent on its deacetylates; Data are means ± standard error of the mean; n = 6 to 8 mice/group. *$P < .05$, **$P < .01$, ***$P < .001$. Similar results were obtained in 3 independent experiments.

University of Chinese Medicine. Hepatic SIRT6-deficient mice were kindly provided by Jinhan He and Yongsheng Chang, and were generated and used as previously described.[21] For inducing hepatic SIRT6 overexpression, mice were injected through the tail vein with 1 to 2 × 10^{9} PFU per adenovirus expressing SIRT6 (Ad-SIRT6, OBiO, Shanghai, China) or adenovirus expressing green fluorescent protein (Ad-Gfp, OBiO, Shanghai, China).[57] To pharmacologically activate SIRT6, MDL-800, a SIRT6 allosteric activator, was intraperitoneally injected twice (100 mg/kg,

24 hours pre and 4 hours post) as previously reported.[58] Nr1h4 knockout (FXR^{-/-}) mice were purchased from Jackson Laboratory and maintained as previously reported.[33] To pharmacologically activate FXR, mice received a daily gavage of OCA (40 mg/kg) for 5 days as previously reported.[3] All mice were kept in 12-hour (light/dark) cycle animal facility with a relative humidity of 50% to 70% and free access to unrestricted food and water. Animal experimental protocols were approved by the Animal Ethics Committee of Guangzhou University of Chinese Medicine
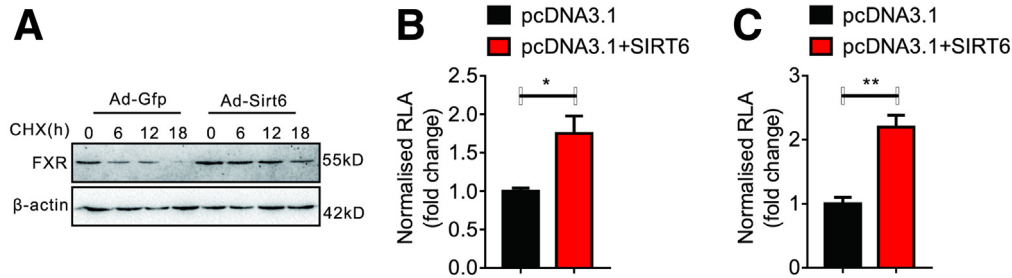
Figure 16. SIRT6 affects the stability and transcriptional activity of FXR. (*A*) Sirt6 overexpression increase the stability of FXR. (*B* and *C*) Sirt6 overexpression increased the trancrptional activity of FXR (*B*) and BSEP (*C*). Data are means ± standard error of the mean; n = 6 to 8 /group. **P* < .05, ***P* < .01.
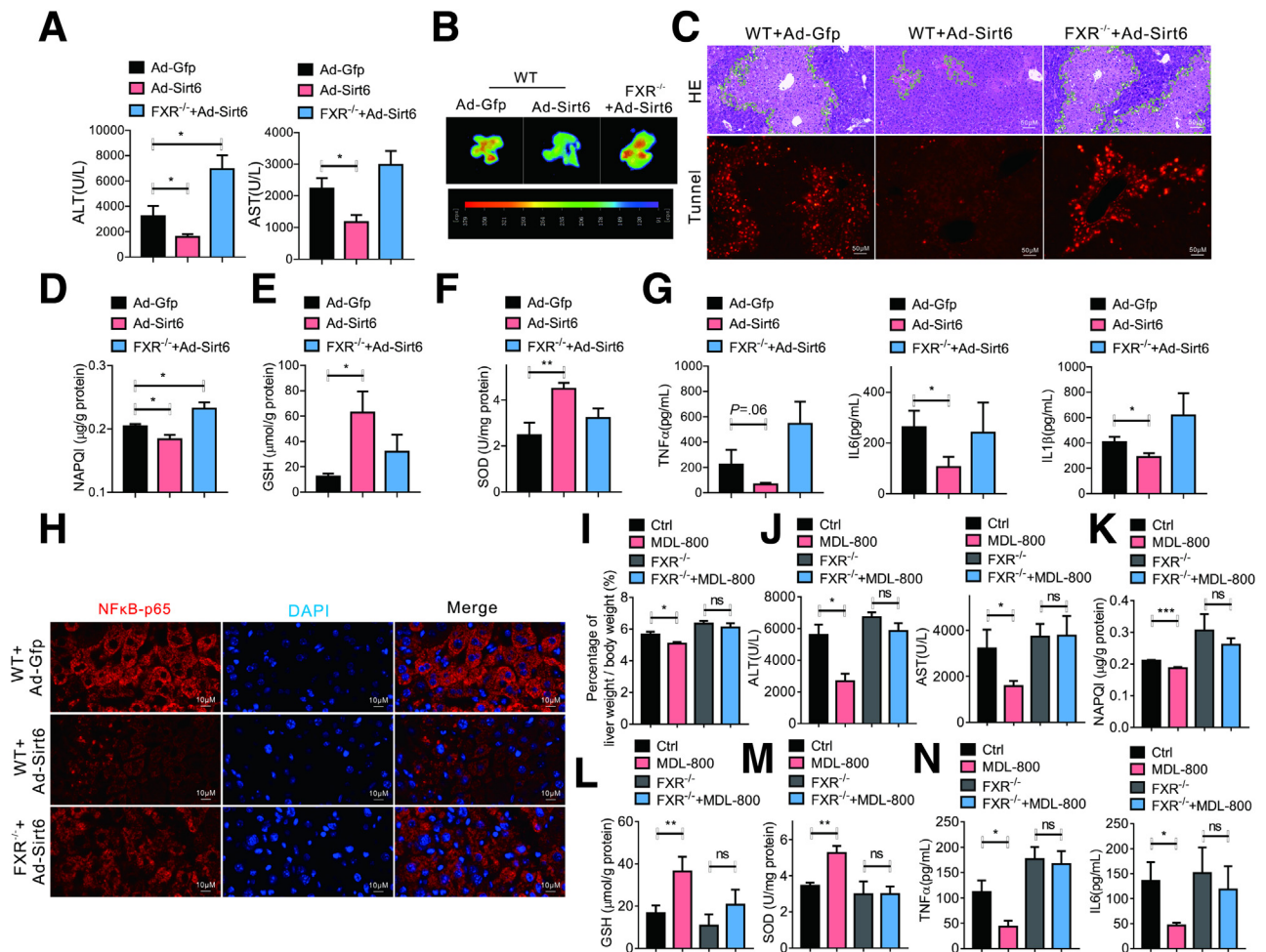

Figure 17. FXR deficiency compromises genetic or pharmacological SIRT6 activation-mediated protective effects against APAP overdose. Occurrences at 12 hours following APAP injection. (*A*) FXR deficiency compromises the effect of SIRT6 on serum ALT and AST alteration; (*B*) SIRT6 overexpression failed to alter hepatic ROS generation in FXR knockout mice; (*C*) FXR knockout reduced the effect of SIRT6 on hepatic centrilobular necrosis and liver cell apoptosis; (*D–F*) The effects of SIRT6 overexpression on the change of NAPQI (*D*), GSH (*E*), and SOD (*F*) levels were weakened in FXR-KO mice; (*G*) FXR knockout abrogated the protective effects of SIRT6 overexpression on serum pro-inflammatory cytokines; (*H*) FXR knockout reduced the effect of SIRT6 on hepatic NF-κBp65 expression; (*I*) The effect of MDL-800 on the ratio of liver weight relative to body weight was diminished in FXR$^{-/-}$ mice; (*J*) The effect of MDL-800 on serum ALT and AST alteration was compromised in FXR$^{-/-}$ mice; (*K–M*) MDL-800 treatment failed to change the hepatic NAPQI (*K*), GSH (*L*), and SOD (*M*) levels in FXR$^{-/-}$ mice; (*N*) MDL-800 treatment did not change the serum pro-inflammatory cytokines in FXR$^{-/-}$ mice. Data are means ± standard error of the mean; n = 6 to 8 mice/group. **P* < .05, ***P* < .01, ****P* < .001. Similar results were obtained in 3 independent experiments.
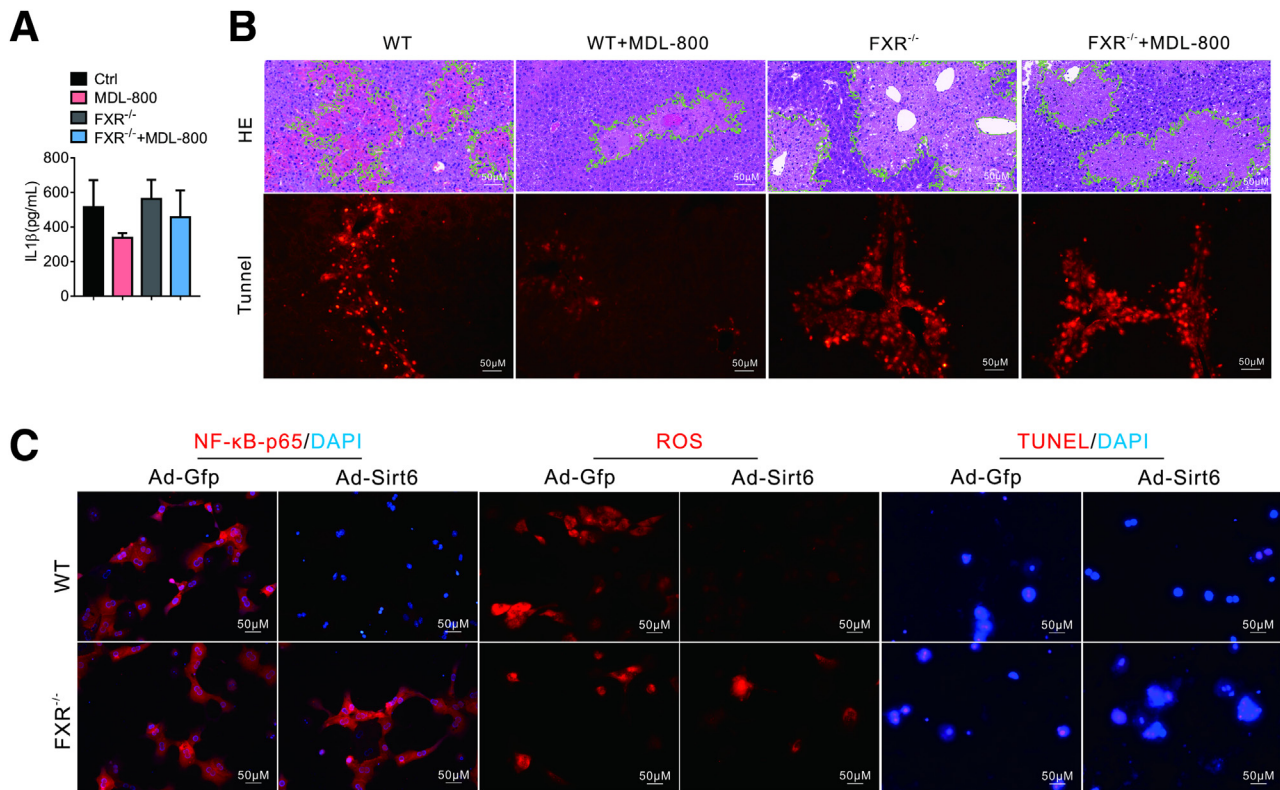
Figure 18. FXR deficiency abrogates genetic or pharmacological SIRT6 activation-mediated protective effects against APAP overdose in vivo and in vitro. (*A*) FXR deficiency compromises the effect of MDL-800 on serum IL-1β alteration; (*B*) FXR knockout reduced the effect of MDL-800 on hepatic centrilobular necrosis and liver cell apoptosis; (*C*) FXR knockout reduced the protective effect of SIRT6 in MPHs. Data are means $\pm$ standard error of the mean; n = 6 to 8 mice/group.

Cell Culture

MPHs were isolated from C57BL/6J or SIRT6$^{alb-/-}$mice as previously described[56] and cultured in RPMI-1640 medium (10% fetal bovine serum, 100 units/mL penicillin, and 0.1 mg/mL streptomycin). Cells were infected with Ad-Gfp or Ad-SIRT6 for 12 hours, followed by exposure to APAP (10 mM) for another 24 hours. The cells were then collected for subsequent analyses.
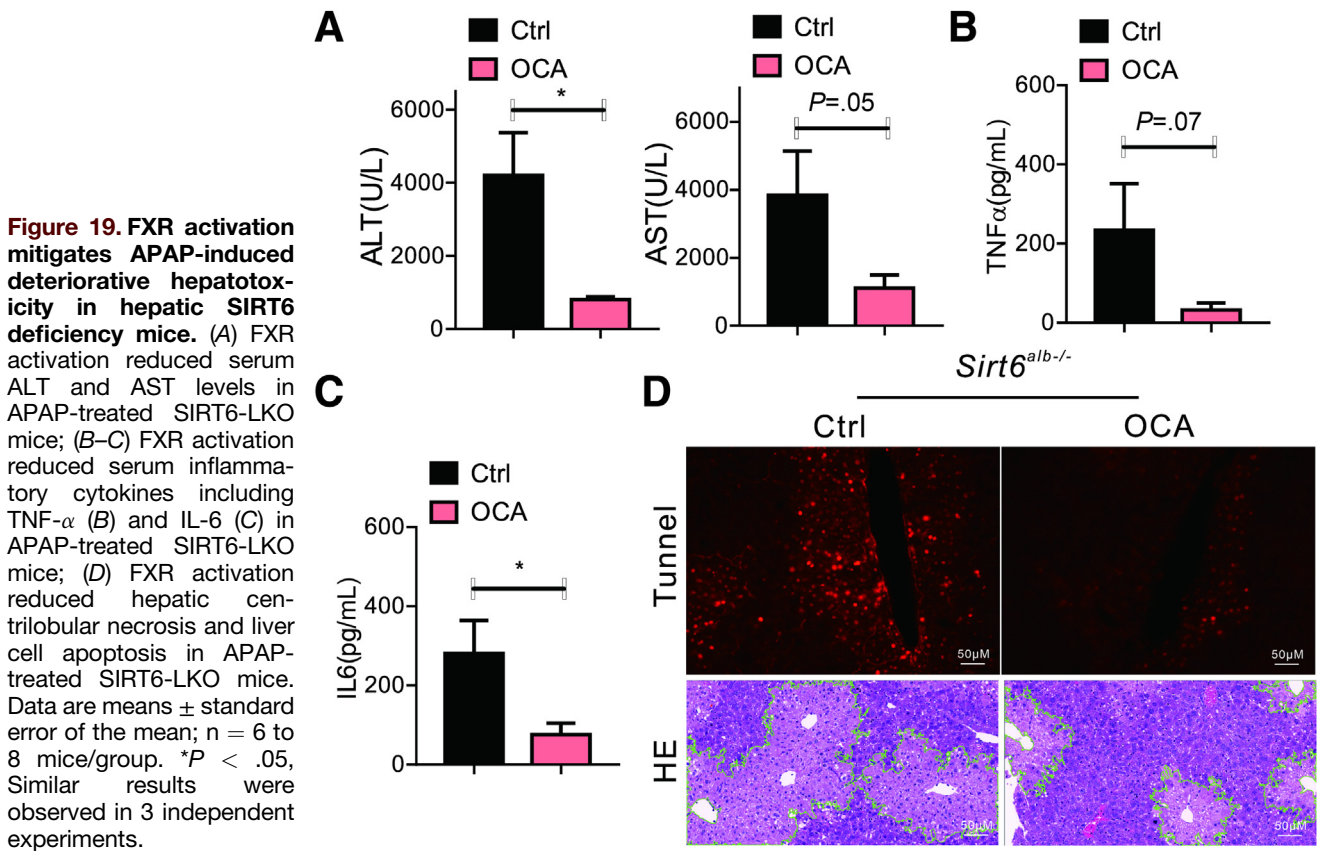
Acetaminophen Treatment

The APAP-induced hepatotoxicity experiments were conducted as previously reported.[33] Briefly, mice were fasted overnight and received 300 mg/kg via intraperitoneal injection, mice were sacrificed 12 hours post APAP injection, and serum and liver tissues were collected for subsequent detection. The survival rate experiments were conducted with a lethal dose of APAP (700 mg/kg), and the death period was recorded within 72 hours. Serum ALT and AST, hepatic GSH, SOD, and NAPQI levels were measured using a reagent kit purchased from Nanjing Jiancheng Bioengineering Institute (Nanjing, China), according to the manufacturer's instructions.

Histology and Immunofluorescence

For hematoxylin and eosin (H&E) staining, liver tissues were fixed in 10% neutral-buffered formalin, embedded in paraffin, and cut into 4-μm sections. Sections were processed for routine H&E staining and examined under a light microscope (Olympus) by an experienced hepatopathologist from the First Affiliated Hospital of Chinese Medicine. Immunofluorescence was performed at Servicebio (Wuhan, China) according to the established protocols. Liver sections or MPHs were incubated with primary antibodies against F4/80 (Santa Cruz), CD11b (Abcam), and FXR (Abcam) at 4 ^{o}C overnight. After being washed 4 times with phosphate-buffered saline (PBS), the sections were incubated with secondary antibodies for 1 hour at 37 ^{o}C. Fluorescence images were obtained using a confocal laser scanning microscope (Leica) or a microscope (Olympus).

TUNEL Assay

MPHs or liver tissues were fixed in 4% paraformaldehyde solution, embedded and frozen, and cut in 30-μm sections by a freezing microtome. TUNEL levels were detected using a TUNEL assay kit (C1089, Beyotime) according to the manufacturer's instructions. Imaging was performed using a fluorescence microscope (Leica Microsystems Ltd, Wetzlar, Germany).

Figure 19. FXR activation mitigates APAP-induced deteriorative hepatotoxicity in hepatic SIRT6 deficiency mice. (*A*) FXR activation reduced serum ALT and AST levels in APAP-treated SIRT6-LKO mice; (*B–C*) FXR activation reduced serum inflammatory cytokines including TNF-α (*B*) and IL-6 (*C*) in APAP-treated SIRT6-LKO mice; (*D*) FXR activation reduced hepatic centrilobular necrosis and liver cell apoptosis in APAP-treated SIRT6-LKO mice. Data are means $\pm$ standard error of the mean; n = 6 to 8 mice/group. *$P < .05$, Similar results were observed in 3 independent experiments.

ROS Determination

ROS levels were measured as previously reported.[56] Briefly, pretreated MPHs were incubated with DHE (5 μM, KeyGENBioTECH) for 30 minutes according to the manufacturer's instructions. The cells were observed under a fluorescence microscope (Olympus, Tokyo, Japan). For hepatic ROS measurement, mice were injected with DHE (10 mM, 10 ul) via the tail vein, and the livers were harvested 1 hour later. ROS levels were measured using Berthold Technologies LB983 NC100.

Enzyme-linked Immunosorbent (ELISA) Assay

Serum or cell culture media levels of inflammatory cytokines including TNF-α, IL-6, and IL-1β, were measured using indicated an ELISA kit according to the manufacturer's instructions (Abclonal, Wuhan, China). Hepatic NAPQI was determined using an ELISA kit from Ruixinbio (Quanzhou, China) following the manufacturer's instructions.

RNA Sequencing

RNA-seq was conducted and analyzed at Berry Genomics Corporation, Beijing, China. Briefly, A total amount of 1 μg RNA from Ad-Gfp- or Ad-Sirt6-infected mice after APAP exposure was used as input material for the RNA sample preparations and NEBNext Ultra RNA Library Prep Kit for Illumina (NEB) was used to conduct sequencing following manufacturer's recommendations. Index codes were added to attribute sequences to each sample. The clustering of the index-coded samples was performed on a cBot Cluster Generation System using TruSeq PE Cluster Kit v3-cBot-HS (Illumia) according to the manufacturer's instructions. After cluster generation, the library preparations were sequenced on an Illumina NovaSeq platform, and 150 bp paired-end reads were generated. Raw data (raw reads) of fastq format were firstly processed through in-house perl scripts. HTSeq v0.6.1 was used to count the reads numbers mapped to each gene, and then FPKM of each gene was calculated based on the length of the gene and reads count mapped to this gene.

Western Blotting

Protein samples from cells or liver tissues were lysed and homogenized in RIPA lysis buffer and protein concentrations were determined using abicinchoninic acid protein assay kit (Beyotime, Biotechnology, Beijing, China). Nuclear and cytoplasmic proteins were extracted using the Nuclear and Cytoplasmic Protein Extraction kit according to the manufacturer's instructions (Beyotime Biotechnology, Beijing, China). In total, 80 to 100 μg of protein were loaded onto a 10% SDS-PAGE gel, and the separated proteins were transferred to polyvinylidene difluoride membranes. Western blot assays were performed using antibodies specific for rabbit anti-Bcl2, rabbit anti-Bax, rabbit anti-SIRT6, mouse anti-β-actin (Abclonal, Wuhan, China), and rabbit anti-NF-κBp65 (Cell Signaling Technology, Danvers, MA).

Protein Interaction and Acetylation Assays

MPHs were harvested and lysed in lysis buffer containing protease inhibitors as previously described. Lysates were immunoprecipitated with anti-SIRT6 (Proteintech)/anti-FXR (Abclonal, Wuhan, China) antibodies or the mouse/rabbit lgG. The total lysates or corresponding immunoprecipitated samples were immunoblotted with anti-SIRT6 and anti-FXR antibodies.

For acetylation assays, Ad-Gfp or Ad-SIRT6 infected MPHs were exposed to APAP (10 mM) treatment for 24 hours. Cells were lysed in lysis buffer containing protease and acetylase inhibitors (Beyotime Biotechnology, Beijing, China). Anti-FXR antibody was used to immunoprecipitate endogenous FXR in protein samples, and acetylated FXR was detected with an acetyl-Lysine antibody (Abclonal, Wuhan, China) using Western blotting.

Quantitative Polymerase Chain Reaction

Total RNA from liver tissues or cells was extracted using TRIzol reagent (Takara) and reverse-transcribed to cDNA using a high-capacity cDNA reverse-transcription kit (Applied Biological Materials Inc, Vancouver, Canada). The resulting cDNA were subjected to quantitative real-time polymerase chain reaction analysis (PowerUpTM SYBRTM Green Master Mix). All gene expressions were normalized to β-actin, and specific primer sequences are shown in Table 1.

Dual-luciferase Reporter Assay

Luciferase reporter assays were performed as previously reported.[33] Briefly, HepG2 cells were cultured in 24-well plates and SIRT6 expressing plasmids (pcDNA3.1-SIRT6) were co-transfected with plasmids containing hFXR-luc or hBSEP-luc into cells, and the pGL3-CMV Renilla luciferase plasmid and, pcDNA3.1-entry vector was used as a control. pcDNA3.1-SIRT6 was generated from Tsingke (Beijing, China). After 48 hours, the cells were harvested, and luciferase activity was measured using the Dual Luciferase Reporter Assay System (Promega). Relative luciferase activity was corrected for Renilla luciferase activity of pCMV-RL-TK and normalized to the activity of the control.

Flow Cytometry Assay

According to the extraction and separation method of primary mouse liver cells described in 2.1, perfusion fluid containing type II collagenase was injected into the inferior vena cava of mice. The liver was removed, added to RPMI 1640 basal medium, ground, and filtered in a cell filter (70 μm) to collect the filtrate. The obtained filtrate was centrifuged again at 1500 rpm × 3 minutes to collect the supernatant ①. PBS was added to the precipitate, mixed, and centrifuged twice at 50g × 3 minutes to collect the supernatant ②. Liquid ① and ②were mixed and centrifuged at 500g × 5 minutes to collect the precipitation. Again, 3 mL PBS was added to the precipitate, and then gently mixed into 3 mL 33% Percoll cell separation solution. The precipitates were collected by centrifugation at room temperature at 1500g × 20 minutes and re-suspended with 200 uL PBS. FITC anti-mouse F4/80 antibody and PE anti-mouse CDllb antibody were added, mixed, and incubated at 4 °C

for 30 minutes under dark conditions. Then, 1 mL PBS containing 5% bovine serum albumin was added and centrifuged at 2000 rpm × 5 minutes to wash the unbound antibodies. The cells were suspended with 500 uL sheath solution and detected by flow cytometry.

Statistical Analysis

Data processing and statistical analysis complied with the previously described recommendations on experimental

Table 1. Primer Information for Gene Amplification

Primer	Sequences
SIRT6(h)	F1: CCCACGGAGTCTGGACCAT R1: CTCTGCCAGTTTGTCCCTG
SIRT6(m)	F1: CTCCAGCGTGGTTTTCCACA R1: GCCCATGCGTTCTAGCTGA
Cyp3a11(m)	F1: CTGGAGGTGATGTTGAGTGTT R1: TGCTAGCCTAAGCATTGGAC
Cyp2e1(m)	F1: CGTTGCCTTGCTTGTCTGGA R1: AAGAAAGGAATTGGGAAAGGTCC
Ugt1a11(m)	F1: TCTGCTTCTTCCGTACCTTCT R1: GCTTCAGGTGCTATGACCACAA
Ostβ(m)	F1: AGATGCGGCTCCTTGGAATTA R1: GGCTGCTTCTTTCGATTTCTG
Ntcp(m)	F1: CAAACCTCAGAAGGACCAAACA R1: GTAGGAGGATTATTCCCGTTGTG
Oatp1a1(m)	F1: GTGCATACCTAGCCAAATCACT R1: CCAGGCCCATAACCACACA
Sod2(m)	F1:CAGACCTGCCTTACGACTATGG R1: CTCGGTGGCGTTGAGATTGTT
Gclc(m)	F1: CTACCACGCAGTCAAGGACC R1: CCTCCATTCAGTAACAACTGGAC
Bcl$_2$(m)	F1: GCTACCGTCGTGACTTCGC R1: CCCCACCGAACTCAAAGAAGG
Bax(m)	F1: AGACAGGGGCCTTTTTGCTAC R1: AATTCGCCGGAGACACTCG
TNFα(m)	F1: CAGGCGGTGCCTATGTCTC R1: CGATCACCCCGAAGTTCAGTAG
IL-6(m)	F1: CTGCAAGAGACTTCCATCCAG R1: AGTGGTATAGACAGGTCTGTTGG
IL-1β(m)	F1: GAAATGCCACCTTTTGACAGTG R1: TGGATGCTCTCATCAGGACAG
Fxr(m)	F1: CAGAAATGGCAACCAGTCATGTA R1: AAATCTCCGCCGAACGAA
Shp(m)	F1: CAGGTCGTCCGACTATTCTGT R1: AGGCTACTGTCTTGGCTAGGA
Bsep(m)	F1: AGCAGGCTCAGCTGCATGAC R1: AATGGCCCGAGCAATAGCAA
Abcc2(m)	F1: GTGTGGATTCCCTTGGGCTTT R1: CACAACGAACACCTGCTTGG
Abcc3(m)	F1: CTGGGTCCCCTGCATCTAC R1: GCCGTCTTGAGCCTGGATAAC
Abcc4(m)	F1: AGGAGCTTCAACGGTACTGG R1: GCCTTTGTTAAGGAGGGCTTC
β-actin(m)	F1: GGCCAACCGTGAAAAGATGA R1: CAGCCTGGATGGCTACGTACA

design and analysis in pharmacology.[61] All results in the figure and text were expressed as means ± standard error of the mean; data were evaluated and statistical differences between groups were assessed using the Student t test and 1-way analysis of variance followed by a post-hoc Tukey test for multiple group comparisons using GraphPad Prism (Version 6.0). The curves of survival rates were analyzed using a repeated-measures 2-way analysis of variance. Statistical significance was set at $P < .05$.

References

1. Larson AM. Acetaminophen hepatotoxicity. Clin Liver Dis 2007;11:525–548, vi.
2. Shan S, Shen Z, Song F. Autophagy and acetaminophen-induced hepatotoxicity. Arch Toxicol 2018;92:2153–2161.
3. Chao X, Wang H, Jaeschke H, Ding WX. Role and mechanisms of autophagy in acetaminophen-induced liver injury. Liver Int 2018;38:1363–1374.
4. Aleksunes LM, Scheffer GL, Jakowski AB, Pruimboom-Brees IM, Manautou JE. Coordinated expression of multidrug resistance-associated proteins (Mrps) in mouse liver during toxicant-induced injury. Toxicol Sci 2006;89:370–379.
5. Pu S, Ren L, Liu Q, Kuang J, Shen J, Cheng S, Zhang Y, Jiang W, Zhang Z, Jiang C, He J. Loss of 5-lipoxygenase activity protects mice against paracetamol-induced liver toxicity. Br J Pharmacol 2016;173:66–76.
6. McGill MR, Sharpe MR, Williams CD, Taha M, Curry SC, Jaeschke H. The mechanism underlying acetaminophen-induced hepatotoxicity in humans and mice involves mitochondrial damage and nuclear DNA fragmentation. J Clin Invest 2012;122:1574–1583.
7. Yan M, Huo Y, Yin S, Hu H. Mechanisms of acetaminophen-induced liver injury and its implications for therapeutic interventions. Redox Biol 2018; 17:274–283.
8. Sanz-Garcia C, Ferrer-Mayorga G, Gonzalez-Rodriguez A, Valverde AM, Martin-Duce A, Velasco-Martin JP, Regadera J, Fernandez M, Alemany S. Sterile inflammation in acetaminophen-induced liver injury is mediated by Cot/tpl2. J Biol Chem 2013; 288:15342–15351.
9. Woolbright BL, Jaeschke H. Role of the inflammasome in acetaminophen-induced liver injury and acute liver failure. J Hepatol 2017;66:836–848.
10. Starkey Lewis P, Campana L, Aleksieva N, Cartwright JA, Mackinnon A, O'Duibhir E, Kendall T, Vermeren M, Thomson A, Gadd V, Dwyer B, Aird R, Man TY, Rossi AG, Forrester L, Park BK, Forbes SJ. Alternatively activated macrophages promote resolution of necrosis following acute liver injury. J Hepatol 2020;73:349–360.
11. Elhanati S, Kanfi Y, Varvak A, Roichman A. Carmel-Gross I, Barth S, Gibor G, Cohen HY. Multiple regulatory layers of SREBP1/2 by SIRT6. Cell Rep 2013;4:905–912.
12. Naiman S, Huynh FK, Gil R, Glick Y, Shahar Y, Touitou N, Nahum L, Avivi MY, Roichman A, Kanfi Y, Gertler AA, Doniger T, Ilkayeva OR, Abramovich I, Yaron O, Lerrer B, Gottlieb E, Harris RA, Gerber D, Hirschey MD, Cohen HY. SIRT6 promotes hepatic beta-oxidation via activation of PPARalpha. Cell Rep 2019;29:4127–4143.e8.
13. Sebastian C, Zwaans BM, Silberman DM, Gymrek M, Goren A, Zhong L, Ram O, Truelove J, Guimaraes AR, Toiber D, Cosentino C, Greenson JK, MacDonald AI, McGlynn L, Maxwell F, Edwards J, Giacosa S, Guccione E, Weissleder R, Bernstein BE, Regev A, Shiels PG, Lombard DB, Mostoslavsky R. The histone deacetylase SIRT6 is a tumor suppressor that controls cancer metabolism. Cell 2012;151:1185–1199.
14. Tang Q, Gao Y, Liu Q, Yang X, Wu T, Huang C, Huang Y, Zhang J, Zhang Z, Li R, Pu S, Zhang G, Zhao Y, Zhou J, Huang H, Li Y, Jiang W, Chang Y, He J. Sirt6 in pro-opiomelanocortin neurons controls energy metabolism by modulating leptin signaling. Mol Metab 2020; 37:100994.
15. Kawahara TL, Michishita E, Adler AS, Damian M, Berber E, Lin M, McCord RA, Ongaigui KC, Boxer LD, Chang HY, Chua KF. SIRT6 links histone H3 lysine 9 deacetylation to NF-kappaB-dependent gene expression and organismal life span. Cell 2009;136:62–74.
16. Pan H, Guan D, Liu X, Li J, Wang L, Wu J, Zhou J, Zhang W, Ren R, Zhang W, Li Y, Yang J, Hao Y, Yuan T, Yuan G, Wang H, Ju Z, Mao Z, Li J, Qu J, Tang F, Liu GH. SIRT6 safeguards human mesenchymal stem cells from oxidative stress by coactivating NRF2. Cell Res 2016; 26:190–205.
17. Zhaohui C, Shuihua W. Protective effects of SIRT6 against inflammation, oxidative stress, and cell apoptosis in spinal cord injury. Inflammation 2020; 43:1751–1758.
18. Hao L, Bang IH, Wang J, Mao Y, Yang JD, Na SY, Seo JK, Choi HS, Bae EJ, Park BH. ERRgamma suppression by Sirt6 alleviates cholestatic liver injury and fibrosis. JCI Insight 2020;5:e137566.
19. Kim HG, Huang M, Xin Y, Zhang Y, Zhang X, Wang G, Liu S, Wan J, Ahmadi AR, Sun Z, Liangpunsakul S, Xiong X, Dong XC. The epigenetic regulator SIRT6 protects the liver from alcohol-induced tissue injury by reducing oxidative stress in mice. J Hepatol 2019; 71:960–969.
20. Liu X, Yang Z, Li H, Luo W, Duan W, Zhang J, Zhu Z, Liu M, Li S, Xin X, Wu H, Xian S, Liu M, Liu C, Shen C. Chrysophanol alleviates metabolic syndrome by activating the SIRT6/AMPK signaling pathway in brown adipocytes. Oxid Med Cell Longev 2020;2020:7374086.
21. Zhang J, Li Y, Liu Q, Huang Y, Li R, Wu T, Zhang Z, Zhou J, Huang H, Tang Q, Huang C, Zhao Y, Zhang G, Jiang W, Mo L, Zhang J, Xie W, He J. Sirt6 Alleviated liver fibrosis by deacetylating conserved lysine 54 on Smad2 in hepatic stellate cells. Hepatology 2021;73:1140–1157.
22. Lu Z, Bourdi M, Li JH, Aponte AM, Chen Y, Lombard DB, Gucek M, Pohl LR, Sack MN. SIRT3-dependent deacetylation exacerbates acetaminophen hepatotoxicity. EMBO Rep 2011;12:840–846.
23. Rada P, Pardo V, Mobasher MA, Garcia-Martinez I, Ruiz L, Gonzalez-Rodriguez A, Sanchez-Ramos C, Muntane J, Alemany S, James LP, Simpson KJ, Monsalve M, Valdecantos MP, Valverde AM. SIRT1 controls acetaminophen hepatotoxicity by modulating

inflammation and oxidative stress. Antioxid Redox Signal 2018;28:1187–1208.

24. Sarikhani M, Mishra S, Desingu PA, Kotyada C, Wolfgeher D, Gupta MP, Singh M, Sundaresan NR. SIRT2 regulates oxidative stress-induced cell death through deacetylation of c-Jun NH2-terminal kinase. Cell Death Differ 2018;25:1638–1656.

25. Zhou Y, Fan X, Jiao T, Li W, Chen P, Jiang Y, Sun J, Chen Y, Chen P, Guan L, Wen Y, Huang M, Bi H. SIRT6 as a key event linking P53 and NRF2 counteracts APAP-induced hepatotoxicity through inhibiting oxidative stress and promoting hepatocyte proliferation. Acta Pharm Sin B 2021;11:89–99.

26. Shin DJ, Wang L. Bile acid-activated receptors: a review on FXR and other nuclear receptors. Handb Exp Pharmacol 2019;256:51–72.

27. Weber AA, Mennillo E, Yang X, van der Schoor LWE, Jonker JW, Chen S, Tukey RH. Regulation of intestinal UDP-glucuronosyltransferase 1A1 by the Farnesoid X receptor agonist obeticholic acid is controlled by constitutive androstane receptor through intestinal maturation. Drug Metab Dispos 2021;49:12–19.

28. Fuchs CD, Traussnigg SA, Trauner M. Nuclear receptor modulation for the treatment of nonalcoholic fatty liver disease. Semin Liver Dis 2016;36:69–86.

29. Liu M, Zhang G, Wu S, Song M, Wang J, Cai W, Mi S, Liu C. Schaftoside alleviates HFD-induced hepatic lipid accumulation in mice via upregulating farnesoid X receptor. J Ethnopharmacol 2020;255:112776.

30. Verbeke L, Farre R, Trebicka J, Komuta M, Roskams T, Klein S, Elst IV, Windmolders P, Vanuytsel T, Nevens F, Laleman W. Obeticholic acid, a farnesoid X receptor agonist, improves portal hypertension by two distinct pathways in cirrhotic rats. Hepatology 2014;59:2286–2298.

31. Xiao Q, Zhang S, Ren H, Du R, Li J, Zhao J, Gao Y, Zhu Y, Huang W. Ginsenoside Rg1 alleviates ANIT-induced intrahepatic cholestasis in rats via activating farnesoid X receptor and regulating transporters and metabolic enzymes. Chem Biol Interact 2020; 324:109062.

32. Lee FY, de Aguiar Vallim TQ, Chong HK, Zhang Y, Liu Y, Jones SA, Osborne TF, Edwards PA. Activation of the farnesoid X receptor provides protection against acetaminophen-induced hepatic toxicity. Mol Endocrinol 2010;24:1626–1636.

33. Liu M, Zhang G, Song M, Wang J, Shen C, Chen Z, Huang X, Gao Y, Zhu C, Lin C, Mi S, Liu C. Activation of farnesoid X receptor by schaftoside ameliorates acetaminophen-induced hepatotoxicity by modulating oxidative stress and inflammation. Antioxid Redox Signal 2020;33:87–116.

34. Yan T, Yan N, Wang H, Yagai T, Luo Y, Takahashi S, Zhao M, Krausz KW, Wang G, Hao H, Gonzalez FJ. FXR-deoxycholic acid-TNF-alpha axis modulates acetaminophen-induced hepatotoxicity. Toxicol Sci 2021;181:273–284.

35. Grootaert MOJ, Finigan A, Figg NL, Uryga AK, Bennett MR. SIRT6 protects smooth muscle cells from senescence and reduces atherosclerosis. Circ Res 2021; 128:474–491.

36. Kim DH, Xiao Z, Kwon S, Sun X, Ryerson D, Tkac D, Ma P, Wu SY, Chiang CM, Zhou E, Xu HE, Palvimo JJ, Chen LF, Kemper B, Kemper JK. A dysregulated acetyl/SUMO switch of FXR promotes hepatic inflammation in obesity. EMBO J 2015;34:184–199.

37. Wolf KK, Wood SG, Allard JL, Hunt JA, Gorman N, Walton-Strong BW, Szakacs JG, Duan SX, Hao Q, Court MH, von Moltke LL, Greenblatt DJ, Kostrubsky V, Jeffery EH, Wrighton SA, Gonzalez FJ, Sinclair PR, Sinclair JF. Role of CYP3A and CYP2E1 in alcohol-mediated increases in acetaminophen hepatotoxicity: comparison of wild-type and Cyp2e1(-/-) mice. Drug Metab Dispos 2007;35:1223–1231.

38. Cheng J, Ma X, Krausz KW, Idle JR, Gonzalez FJ. Rifampicin-activated human pregnane X receptor and CYP3A4 induction enhance acetaminophen-induced toxicity. Drug Metab Dispos 2009;37:1611–1621.

39. Aleksunes LM, Slitt AL, Maher JM, Augustine LM, Goedken MJ, Chan JY, Cherrington NJ, Klaassen CD, Manautou JE. Induction of Mrp3 and Mrp4 transporters during acetaminophen hepatotoxicity is dependent on Nrf2. Toxicol Appl Pharmacol 2008;226:74–83.

40. Koenderink JB, van den Heuvel J, Bilos A, Vredenburg G, Vermeulen NPE, Russel FGM. Human multidrug resistance protein 4 (MRP4) is a cellular efflux transporter for paracetamol glutathione and cysteine conjugates. Arch Toxicol 2020;94:3027–3032.

41. He J, Zhang G, Pang Q, Yu C, Xiong J, Zhu J, Chen F. SIRT6 reduces macrophage foam cell formation by inducing autophagy and cholesterol efflux under ox-LDL condition. FEBS J 2017;284:1324–1337.

42. Court MH, Freytsis M, Wang X, Peter I, Guillemette C, Hazarika S, Duan SX, Greenblatt DJ, Lee WM. Acute Liver Failure Study Group. The UDP-glucuronosyltransferase (UGT) 1A polymorphism c.2042C>G (rs8330) is associated with increased human liver acetaminophen glucuronidation, increased UGT1A exon 5a/5b splice variant mRNA ratio, and decreased risk of unintentional acetaminophen-induced acute liver failure. J Pharmacol Exp Ther 2013;345:297–307.

43. McGill MR, Jaeschke H. Metabolism and disposition of acetaminophen: recent advances in relation to hepatotoxicity and diagnosis. Pharm Res 2013;30:2174–2187.

44. Wang H, Zhang R, Zhu Y, Teng T, Cheng Y, Chowdhury A, Lu J, Jia Z, Song J, Yin X, Sun Y. Microsomal prostaglandin E synthase 2 deficiency is resistant to acetaminophen-induced liver injury. Arch Toxicol 2019;93:2863–2878.

45. Triantafyllou E, Pop OT, Possamai LA, Wilhelm A, Liaskou E, Singanayagam A, Bernsmeier C, Khamri W, Petts G, Dargue R, Davies SP, Tickle J, Yuksel M, Patel VC, Abeles RD, Stamataki Z, Curbishley SM, Ma Y, Wilson ID, Coen M, Woollard KJ, Quaglia A, Wendon J, Thursz MR, Adams DH, Weston CJ, Antoniades CG. MerTK expressing hepatic macrophages promote the resolution of inflammation in acute liver failure. Gut 2018;67:333–347.

46. Zhong X, Huang M, Kim HG, Zhang Y, Chowdhury K, Cai W, Saxena R, Schwabe RF, Liangpunsakul S, Dong XC. SIRT6 protects against liver fibrosis by deacetylation and suppression of SMAD3 in hepatic

stellate cells. Cell Mol Gastroenterol Hepatol 2020;
10:341–364.

47. Santos-Barriopedro I, Bosch-Presegue L, Marazuela-Duque A, de la Torre C, Colomer C, Vazquez BN, Fuhrmann T, Martinez-Pastor B, Lu W, Braun T, Bober E, Jenuwein T, Serrano L, Esteller M, Chen Z, Barcelo-Batllori S, Mostoslavsky R, Espinosa L, Vaquero A. SIRT6-dependent cysteine monoubiquitination in the PRE-SET domain of Suv39h1 regulates the NF-kappaB pathway. Nat Commun 2018;9:101.

48. Lu Y, Zheng W, Lin S, Guo F, Zhu Y, Wei Y, Liu X, Jin S, Jin L, Li Y. Identification of an oleanane-type triterpene hedragonic acid as a novel farnesoid X receptor ligand with liver protective effects and anti-inflammatory activity. Mol Pharmacol 2018;93:63–72.

49. Gai Z, Visentin M, Gui T, Zhao L, Thasler WE, Hausler S, Hartling I, Cremonesi A, Hiller C, Kullak-Ublick GA. Effects of farnesoid X receptor activation on arachidonic acid metabolism, NF-kB signaling, and hepatic inflammation. Mol Pharmacol 2018;94:802–811.

50. Wang YD, Chen WD, Wang M, Yu D, Forman BM, Huang W. Farnesoid X receptor antagonizes nuclear factor kappaB in hepatic inflammatory response. Hepatology 2008;48:1632–1643.

51. Chen L, Liu Q, Tang Q, Kuang J, Li H, Pu S, Wu T, Yang X, Li R, Zhang J, Zhang Z, Huang Y, Li Y, Zou M, Jiang W, Li T, Gong M, Zhang L, Wang H, Qu A, Xie W, He J. Hepatocyte-specific Sirt6 deficiency impairs ketogenesis. J Biol Chem 2019;294:1579–1589.

52. Zhu L, Wang L, Cao F, Liu P, Bao H, Yan Y, Dong X, Wang D, Wang Z, Gong P. Modulation of transport and metabolism of bile acids and bilirubin by chlorogenic acid against hepatotoxicity and cholestasis in bile duct ligation rats: involvement of SIRT1-mediated deacetylation of FXR and PGC-1alpha. J Hepatobiliary Pancreat Sci 2018;25:195–205.

53. Kazgan N, Metukuri MR, Purushotham A, Lu J, Rao A, Lee S, Pratt-Hyatt M, Lickteig A, Csanaky IL, Zhao Y, Dawson PA, Li X. Intestine-specific deletion of SIRT1 in mice impairs DCoH2-HNF-1alpha-FXR signaling and alters systemic bile acid homeostasis. Gastroenterology 2014;146:1006–1016.

54. Purushotham A, Xu Q, Lu J, Foley JF, Yan X, Kim DH, Kemper JK, Li X. Hepatic deletion of SIRT1 decreases hepatocyte nuclear factor 1alpha/farnesoid X receptor signaling and induces formation of cholesterol gallstones in mice. Mol Cell Biol 2012;32:1226–1236.

55. Kemper JK, Xiao Z, Ponugoti B, Miao J, Fang S, Kanamaluru D, Tsang S, Wu SY, Chiang CM, Veenstra TD. FXR acetylation is normally dynamically regulated by p300 and SIRT1 but constitutively elevated in metabolic disease states. Cell Metab 2009;10:392–404.

56. Sun N, Shen C, Zhang L, Wu X, Yu Y, Yang X, Yang C, Zhong C, Gao Z, Miao W, Yang Z, Gao W, Hu L, Williams K, Liu C, Chang Y, Gao Y. Hepatic Kruppel-like factor 16 (KLF16) targets PPARalpha to improve steatohepatitis and insulin resistance. Gut 2021;70:2183–2195.

57. Yang X, Chen Q, Sun L, Zhang H, Yao L, Cui X, Gao Y, Fang F, Chang Y. KLF10 transcription factor regulates

hepatic glucose metabolism in mice. Diabetologia 2017;
60:2443–2452.

58. Huang Z, Zhao J, Deng W, Chen Y, Shang J, Song K, Zhang L, Wang C, Lu S, Yang X, He B, Min J, Hu H, Tan M, Xu J, Zhang Q, Zhong J, Sun X, Mao Z, Lin H, Xiao M, Chin YE, Jiang H, Xu Y, Chen G, Zhang J. Identification of a cellularly active SIRT6 allosteric activator. Nat Chem Biol 2018;14:1118–1126.

59. Kilkenny C, Browne W, Cuthill IC, Emerson M, Altman DG. NC3Rs Reporting Guidelines Working Group. Animal research: reporting in vivo experiments: the ARRIVE guidelines. Br J Pharmacol 2010;160:1577–1579.

60. McGrath JC, Lilley E. Implementing guidelines on reporting research using animals (ARRIVE etc.): new requirements for publication in BJP. Br J Pharmacol 2015; 172:3189–3193.

61. Curtis MJ, Bond RA, Spina D, Ahluwalia A, Alexander SP, Giembycz MA, Gilchrist A, Hoyer D, Insel PA, Izzo AA, Lawrence AJ, MacEwan DJ, Moon LD, Wonnacott S, Weston AH, McGrath JC. Experimental design and analysis and their reporting: new guidance for publication in BJP. Br J Pharmacol 2015;172:3461–3471.

Correspondence
Address correspondence to: Yong Gao, PhD, 12 Ji Chang Rd, Bai Yun District, Guangzhou, China. e-mail: gaoyong@gzucm.edu.cn; Sheng Lin, PhD, 5 Hai Yun Cang Beijing, China. e-mail: lsznn@126.com; Chong Zhong, MD, 16 Ji Chang Rd, Bai Yun District, Guangzhou, China. e-mail: zhongchong1732@gzucm.edu.cn; or Zifeng Yang, PhD, 195 Dong feng xi Rd, Yue Xiu District Guangzhou, China. e-mail: jeffyah@163.com; fax: 83395651.